CNA activities for the CMS high luminosity upgrade and ECFA DRDs

M.C. Jiménez Ramos, Javier García López, Carmen Torres Muñoz, Mauricio Rodríguez Ramos, Jairo Villegas Domínguez

System upgrades for enhanced microprobe performance Activity WP5.T1.

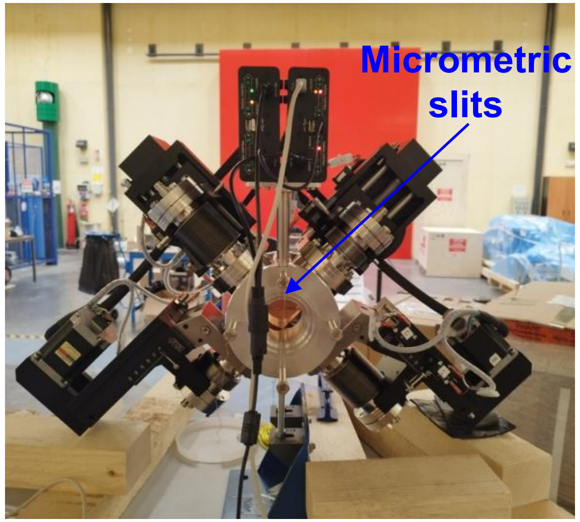

- Integrated a remote-controlled 4-blade micrometric slit system (0.7 μm resolution) to optimize beam geometry and minimize aberrations for IBIC.

- Enables automated, high-precision beam characterization and adjustment without manual intervention, maximizing experimental reproducibility and flexibility.

- Installed a modular lens system and 5 MPx camera for real-time, non-destructive sample observation at the ion beam nuclear microprobe.

- Delivers up to 10X magnification and 12.5:1 zoom, essential for precise beam focusing and accurate targeting of sample regions of interest.

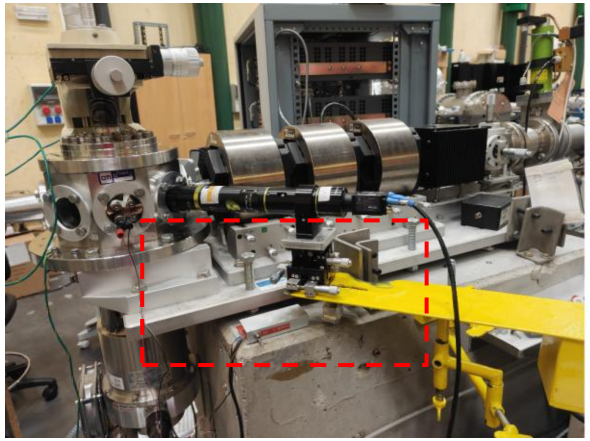

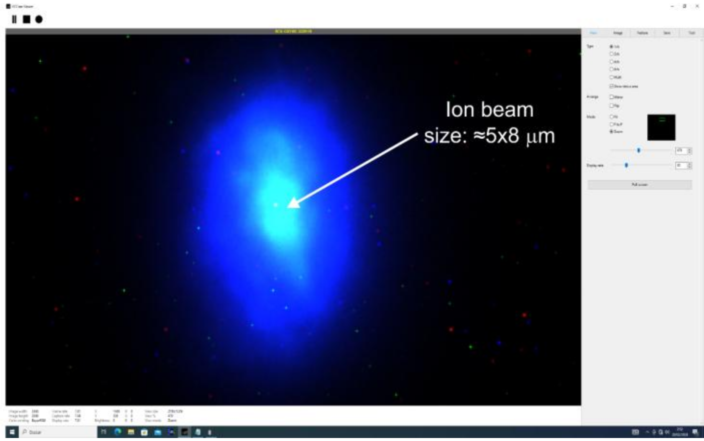

IBIC validation of TPA-TCT method on Silicon Carbide devices (Activity WP5.T3)

TPA-TCT

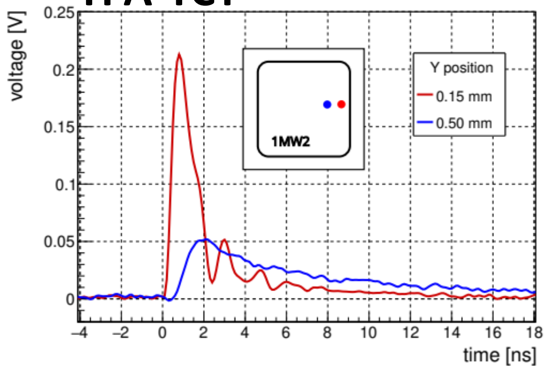

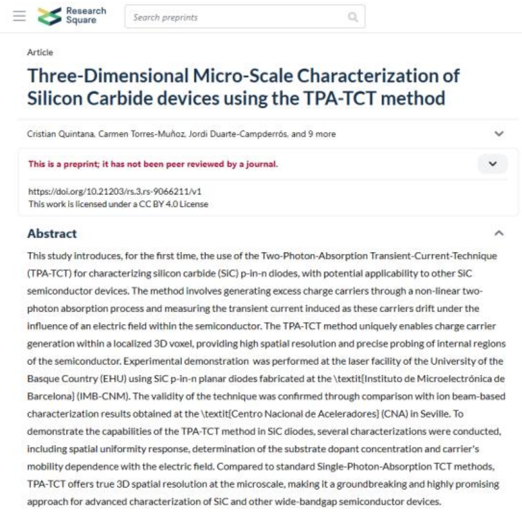

https://www.researchsquare.com/article/rs-9066211/v1

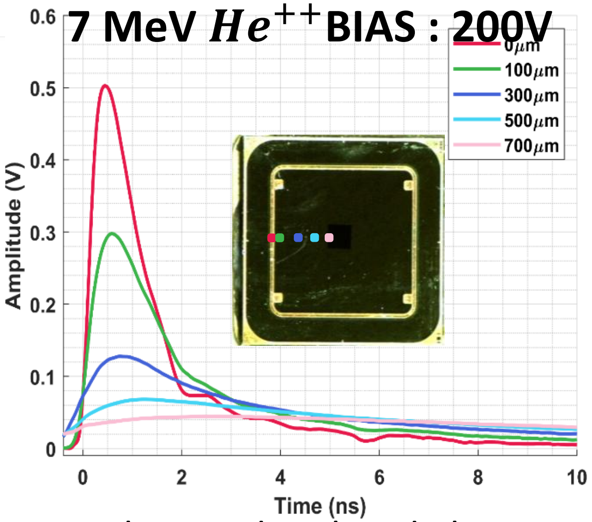

Signals varied with radial position, with signals at the edges being faster and those in the center slower.

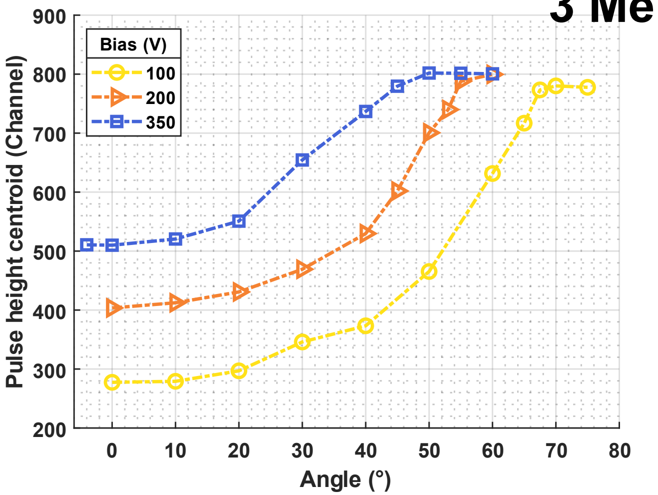

3 MeV H^+

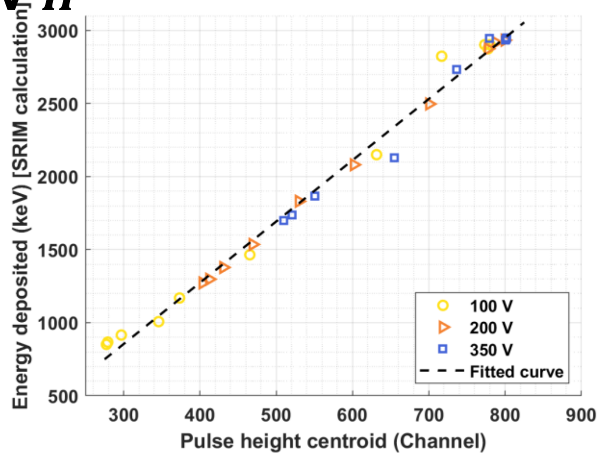

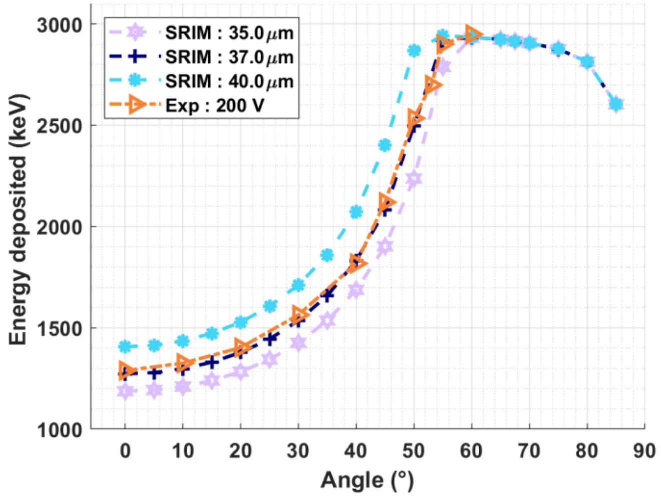

- Theoretical deposited energy (SRIM) for each W and rotation angle
- The results obtained with the IBIC techniques are compatible and confirm the results obtained with the TPA-TCT technique.

Bias voltage (V)	W_{TPA} (μm)	W_{IBIC} (μm)
100	29 ±2	26 ±1
200	36 ±2	37 ±1
350	44 ±2	45 ±1

Carrier Transport Properties of Neutron-Irradiated 4H-SiC (Activity WP3.T2)

Carrier Transport Properties of Neutron-Irradiated 4H-SiC

C. Torres-Muñoz[1], C. Quintana[2], M. Rodríguez-Ramos[1], J. García Lopéz[1,4], J. Duarte-Campderrós[2], D. Rosich[2], I. Vila[2], Marcos Fernández-García[2], Joan Marc Rafí[5], Gemma Rius[5], Ivan López-Paz[5], Giulio Pellegrini[5], and M.C. Jiménez-Ramos[1,3]

[1]Centro Nacional de Aceleradores (CNA) (Universidad de Sevilla, CSIC, Junta de Andalucía)
[2]Instituto de Física de Cantabria (CSIC-UC), E-39005 Santander , Spain
[3]Departamento de Fisica Aplicada II, Universidad de Sevilla, E-41012 Sevilla, Spain
[4]Departamento de Fisica Atomica, Molecular y Nuclear, Universidad de Sevilla, E-41012 Sevilla, Spain
[5]Instituto de Microelectrónica de Barcelona, IMB-CNM (CSIC), Calle de los Tilon s/n, E-08193 Bellaterra, Spain

ABSTRACT

This study investigates the impact of neutron irradiation on the carrier transport properties of 4H-SiC p-on-n diodes at fluences of 4×10^{14} and 1×10^{15} n_{eq}/cm^2. Using a combination of alpha-particle spectrometry, ion-beam induced charge measurements, and depth-resolved laser transient current technique (TCT), we evaluate their degradation of charge collection efficiency and energy resolution. Electrical measurements indicate that irradiation-induced defects compensate the space charge, causing the epitaxial layer to behave as an intrinsic semiconductor material with a nearly uniform electric field. Both ion- and laser-based probing reveal clear asymmetries in carrier transport, where holes are significantly more prone to trapping than electrons. We also report the first application of the Two-Photon Absorption to neutron-irradiated SiC, as an advanced mode of TCT , and detailing a method to suppress radiation-induced background signals. These findings provide essential quantitative data for the development of radiation-hard silicon carbide detectors in high-luminosity particle physics and nuclear environments.

Article draft shared with co-author.
Expected submission: Aug–Sep.

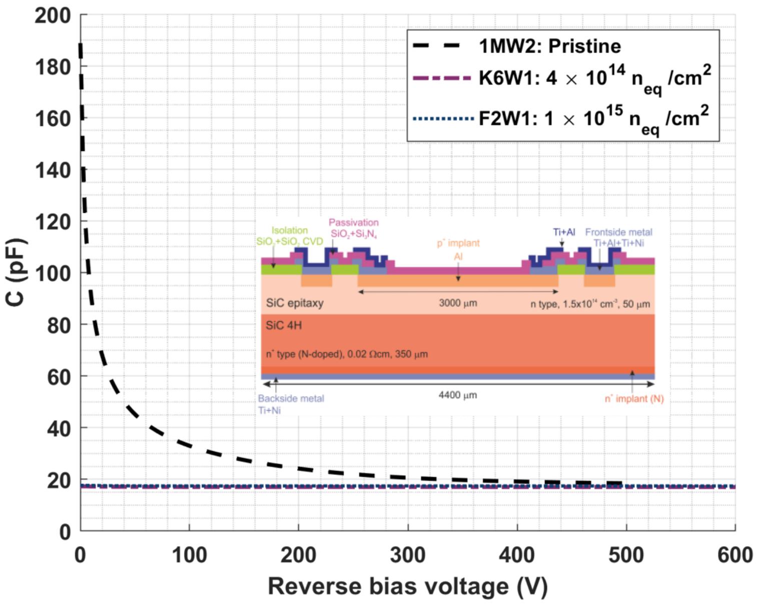

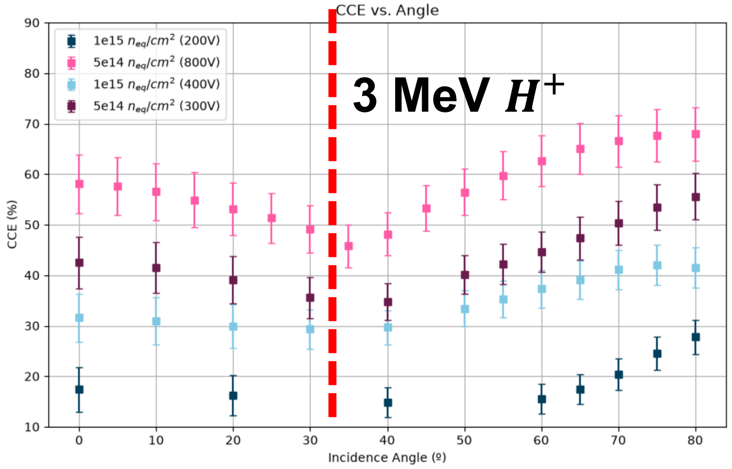

1. Neutron irradiation generates uniform distribution of defects
2. Uniform electric field across the active region (C-V measurements)

Hecht equation ($L_{drift} = (\mu\tau) \cdot E = cte$) [1]

$$\mathrm{CCE(drift)} = \frac{1}{E_0}\int_0^{w} \frac{dE}{dx}\,dx \left[\frac{L_{e^-}}{w}\left(1 - e^{-\frac{w-x}{L_{e^-}}}\right) + \frac{L_{h^+}}{w}\left(1 - e^{-\frac{x}{L_{h^+}}}\right)\right]$$

Each angle produces a different ionization profile (SRIM simulation)

Carrier transport modeled by fitting experimental data using minimization of χ

Fit parameters: electron and hole drift lengths (L_{e^-}, L_{h^+})

$$\chi(L_{e^-}, L_{h^+}) = \sum_{i=1}^{N}\left[\frac{CCE_{exp}(i) - CCE_{model}(i)}{CCE_{exp}(i)}\right]^2$$

[1] J. Garcia Lopez et al., Nucl. Instrum. Methods B, 371 (2016) 294-297.https://doi.org/10.1016/j.nimb.2015.09.012

Carrier Transport Properties of Neutron-Irradiated 4H-SiC (Activity WP3.T2)

Centro Nacional de Aceleradores
INFRAESTRUCTURAS CIENTÍFICAS Y TÉCNICAS SINGULARES

$$\chi(L_{e-}, L_{h+}) = \sum_{i=1}^{N} \left[\frac{CCE_{exp}(i) - CCE_{model}(i)}{CCE_{exp}(i)}\right]^2$$

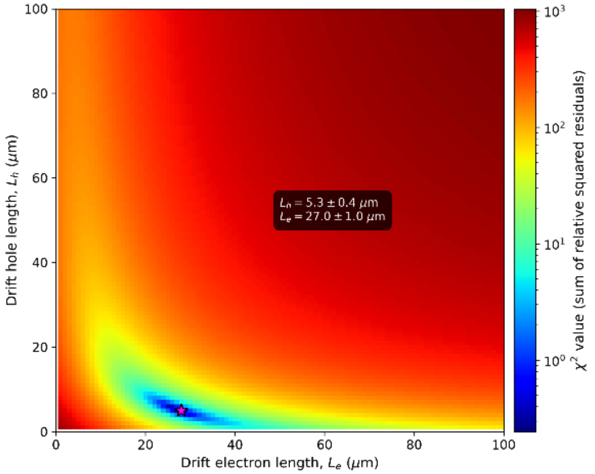

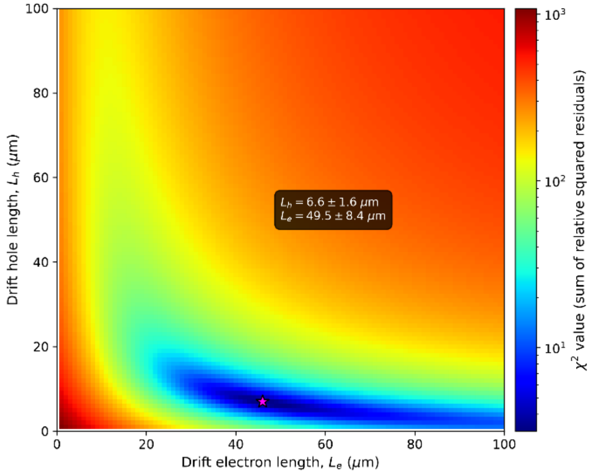

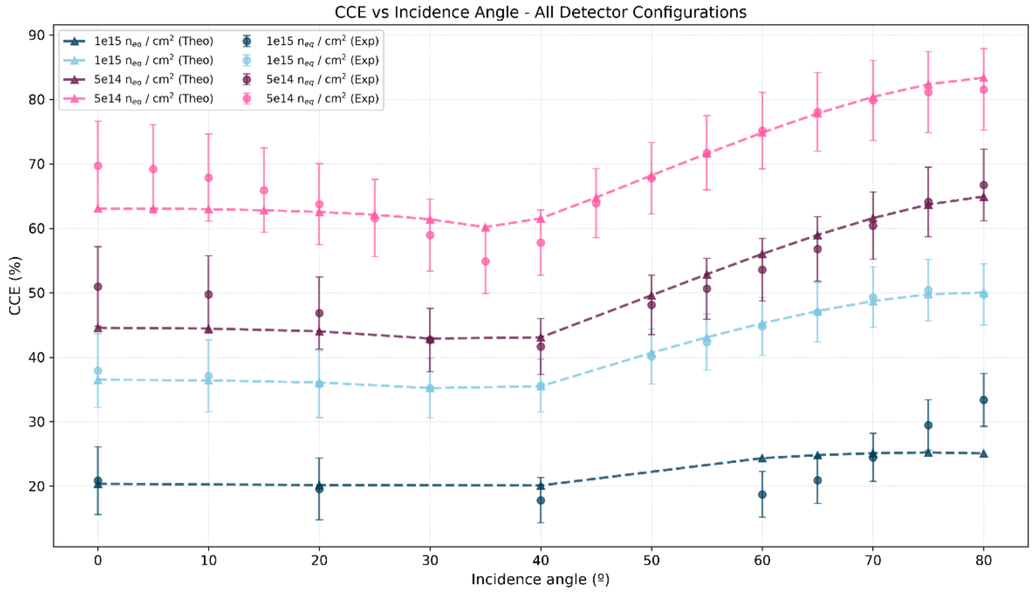

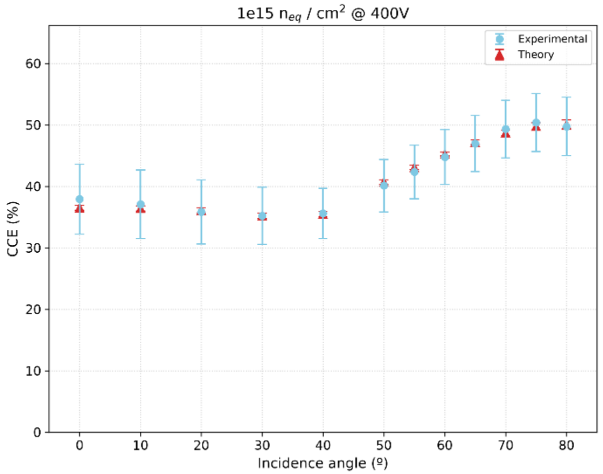

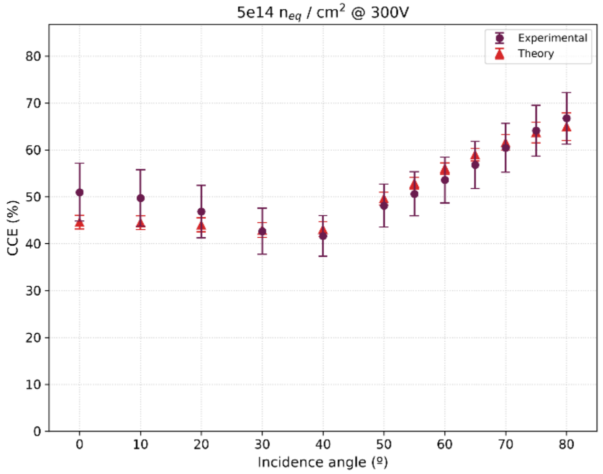

$Fluence (n_{eq}/cm^2)$	V (V)	L_{e^-} (μm)	L_{h^+} (μm)
5×10^{14}	800	130 ± 40	17 ± 3
5×10^{14}	300	50 ± 8	6.6 ± 1.6
1×10^{15}	400	27.0 ± 1.0	5.3 ± 0.4
1×10^{15}	200	11 ± 2	2.3 ± 1.3

Electron drift lengths are consistently 5–8× higher than hole drift lengths across all tested conditions.

Effect of dynamic annealing on 4H-SiC detectors irradiated at different temperatures (Activity WP3.T2)

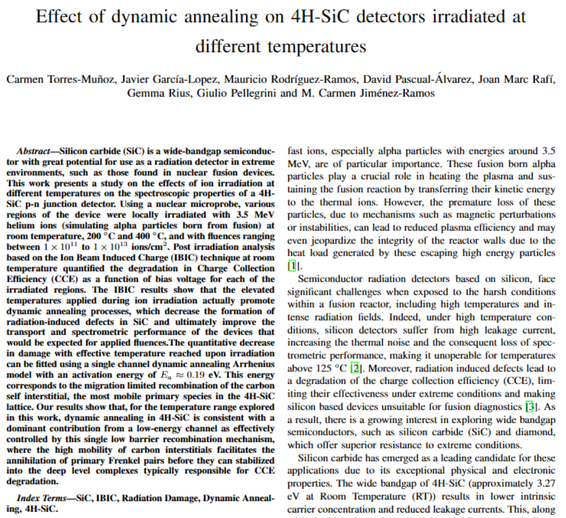

Effect of dynamic annealing on 4H-SiC detectors irradiated at different temperatures

Carmen Torres-Muñoz, Javier García-Lopez, Mauricio Rodríguez-Ramos, David Pascual-Álvarez, Joan Marc Rafí, Gemma Rius, Giulio Pellegrini and M. Carmen Jiménez-Ramos

***Abstract*—Silicon carbide (SiC) is a wide-bandgap semiconductor with great potential for use as a radiation detector in extreme environments, such as those found in nuclear fusion devices. This work presents a study on the effects of ion irradiation at different temperatures on the spectroscopic properties of a 4H-SiC p-n junction detector. Using a nuclear microprobe, various regions of the device were locally irradiated with 3.5 MeV helium ions (simulating alpha particles born from fusion) at room temperature, 200 °C and 400 °C, and with fluences ranging between 1×10^{11} to 1×10^{13} ions/cm². Post irradiation analysis based on the Ion Beam Induced Charge (IBIC) technique at room temperature quantified the degradation in Charge Collection Efficiency (CCE) as a function of bias voltage for each of the irradiated regions. The IBIC results show that the elevated temperatures applied during ion irradiation actually promote dynamic annealing processes, which decrease the formation of radiation-induced defects in SiC and ultimately improve the transport and spectrometric performance of the devices that would be expected for applied fluences.The quantitative decrease in damage with effective temperature reached upon irradiation can be fitted using a single channel dynamic annealing Arrhenius model with an activation energy of $E_a \approx 0.19$ eV. This energy corresponds to the migration limited recombination of the carbon self interstitial, the most mobile primary species in the 4H-SiC lattice. Our results show that, for the temperature range explored in this work, dynamic annealing in 4H-SiC is consistent with a dominant contribution from a low-energy channel as effectively controlled by this single low barrier recombination mechanism, where the high mobility of carbon interstitials facilitates the annihilation of primary Frenkel pairs before they can stabilized into the deep level complexes typically responsible for CCE degradation.**

***Index Terms*—SiC, IBIC, Radiation Damage, Dynamic Annealing, 4H-SiC.**

fast ions, especially alpha particles with energies around 3.5 MeV, are of particular importance. These fusion born alpha particles play a crucial role in heating the plasma and sustaining the fusion reaction by transferring their kinetic energy to the thermal ions. However, the premature loss of these particles, due to mechanisms such as magnetic perturbations or instabilities, can lead to reduced plasma efficiency and may even jeopardize the integrity of the reactor walls due to the heat load generated by these escaping high energy particles [1].

Semiconductor radiation detectors based on silicon, face significant challenges when exposed to the harsh conditions within a fusion reactor, including high temperatures and intense radiation fields. Indeed, under high temperature conditions, silicon detectors suffer from high leakage current, increasing the thermal noise and the consequent loss of spectrometric performance, making it unoperable for temperatures above 125 °C [2]. Moreover, radiation induced defects lead to a degradation of the charge collection efficiency (CCE), limiting their effectiveness under extreme conditions and making silicon based devices unsuitable for fusion diagnostics [3]. As a result, there is a growing interest in exploring wide bandgap semiconductors, such as silicon carbide (SiC) and diamond, which offer superior resistance to extreme conditions.

Silicon carbide has emerged as a leading candidate for these applications due to its exceptional physical and electronic properties. The wide bandgap of 4H-SiC (approximately 3.27 eV at Room Temperature (RT)) results in lower intrinsic carrier concentration and reduced leakage currents. This, along

First review completed
Waiting decision from IEEE Transactions on Instrumentation & Measurement.

3.5 MeV He^{++}

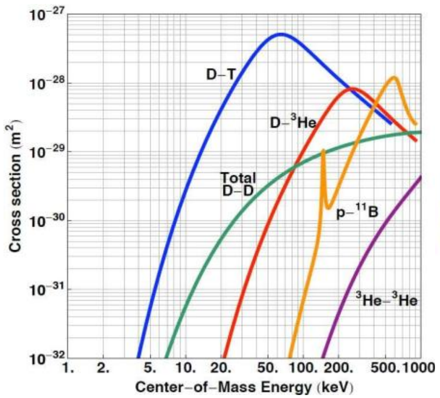

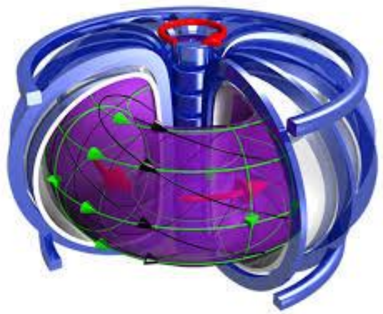

$$^{2}_{1}D + ^{3}_{1}T \rightarrow ^{4}_{2}\mathbf{He} + ^{1}_{0}n + 17.6\ MeV$$

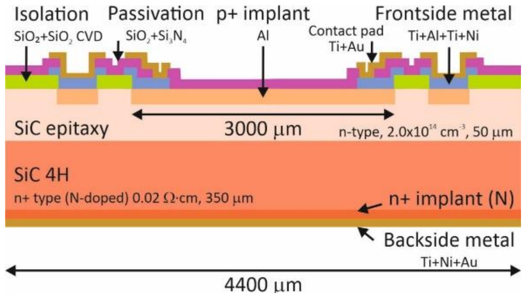

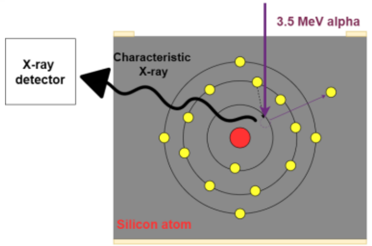

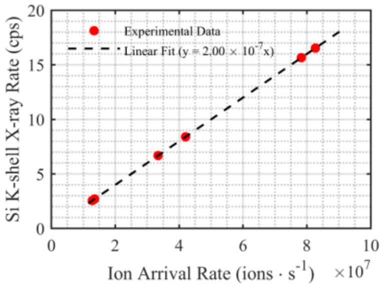

1.Controlled damage of micrometric areas using the ion beam nuclear microprobe at high temperature

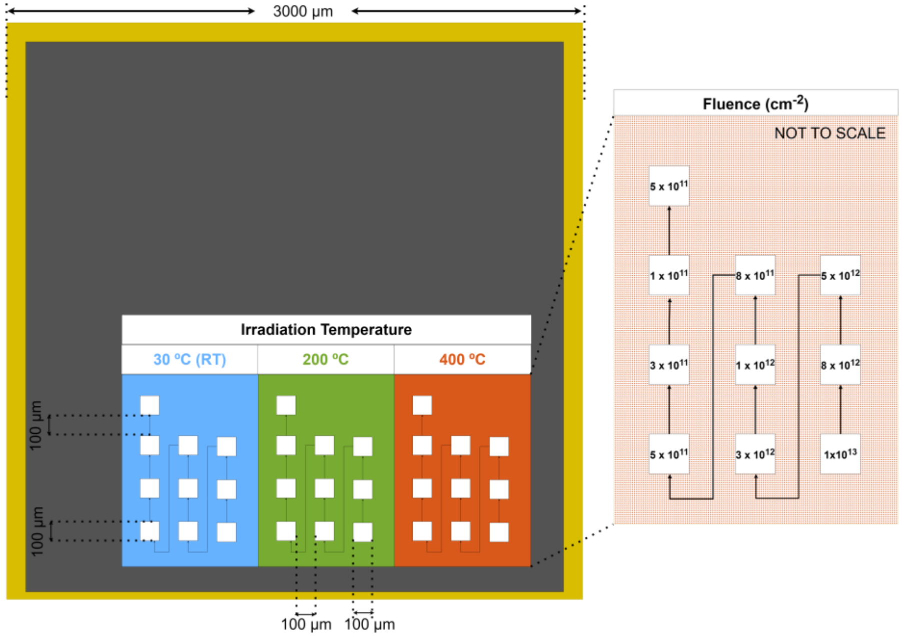

To avoid thermal annealing effects that might occur during high-temperature irradiation, we followed a strict order: starting from **the highest temperature and highest fluence**, then moving to **lower fluences and temperatures**.

Effect of dynamic annealing on 4H-SiC detectors irradiated at different temperatures (Activity WP3.T2)

Centro Nacional de Aceleradores | INFRAESTRUCTURAS CIENTÍFICAS Y TÉCNICAS SINGULARES | Universidad de Sevilla

2. Characterization at RT using ions (IBIC)

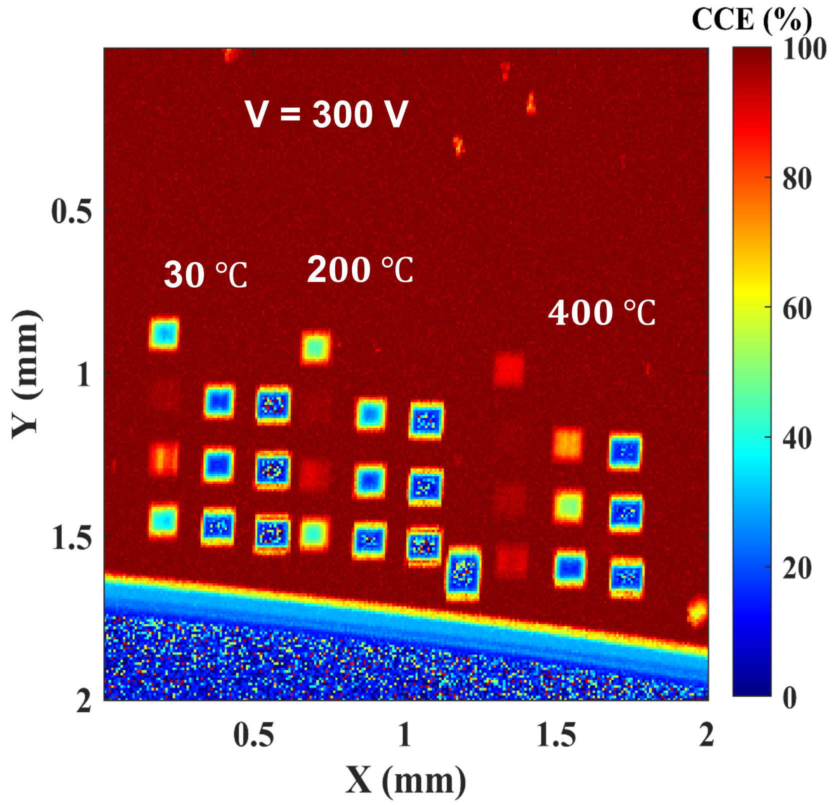

3.5 MeV He^{++}

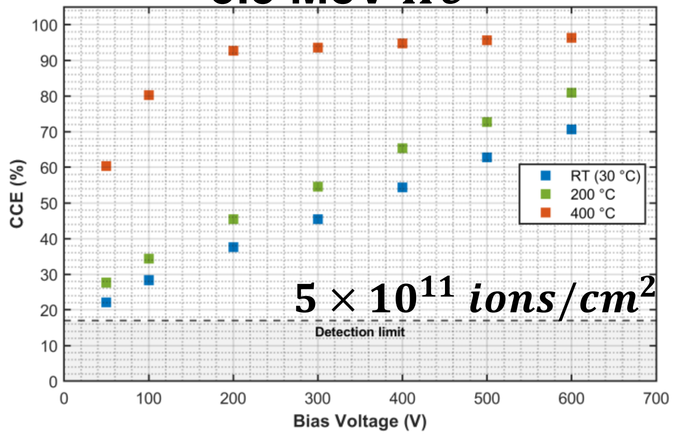

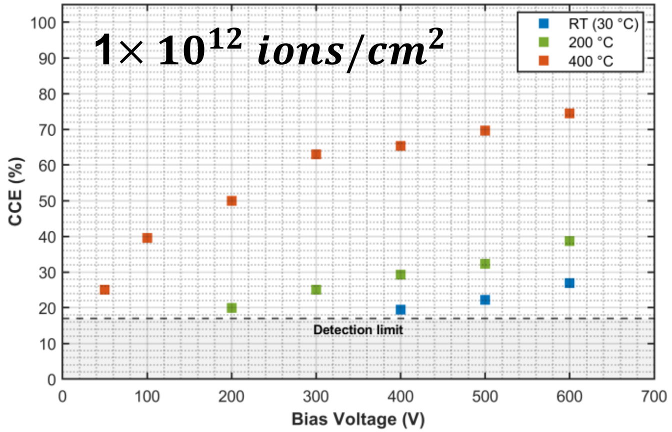

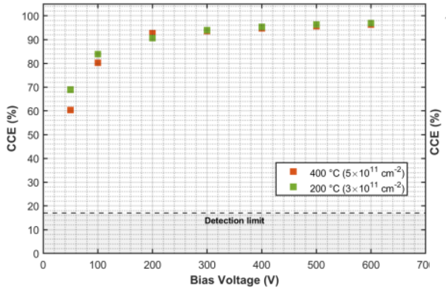

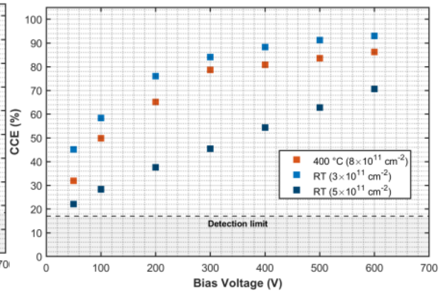

$$CCE\ (400ºC) \gg CCE(200ºC) \gg CCE(RT)$$
$$CCE\ (\downarrow\ fluence) \gg CCE(\uparrow fluence)$$

CCE is significantly better preserved when the irradiations are performed at higher temperatures due to **dynamic anneling**

Some CCE curves **coincide** for different fluences and temperatures.
This enables a quantitative comparison of relative damage severity

$$\frac{N_{30}}{N_{400}} \approx 2.2\ ;\ \frac{N_{200}}{N_{400}} \approx 1.7\ ;\ \frac{N_{30}}{N_{200}} \approx 1.3$$

Kinetic Model: Steady-state balance
(competing stabilization versus thermal recombination)

$$\eta(T) = \frac{\eta_0}{1 + C\exp(-\frac{E_a}{kT})}$$

Markov chain Monte Carlo analysis :
$E_a = 0.19$ eV(0.16−−0.23) and $C = 32$(20−−58)
Physical Mechanism: Single activated process consistent with dynamic annealing driven by **carbon self-interstitial migration.**

LIGHT-ENHANCED RESPONSE IN IRRADIATED DEVICES

After damage at RT and 400°C, the detector response was tested at RT under both dark and blue-LED conditions.

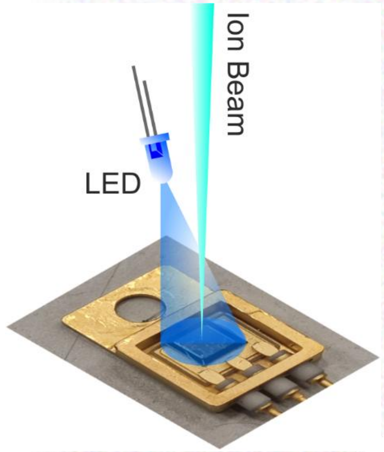

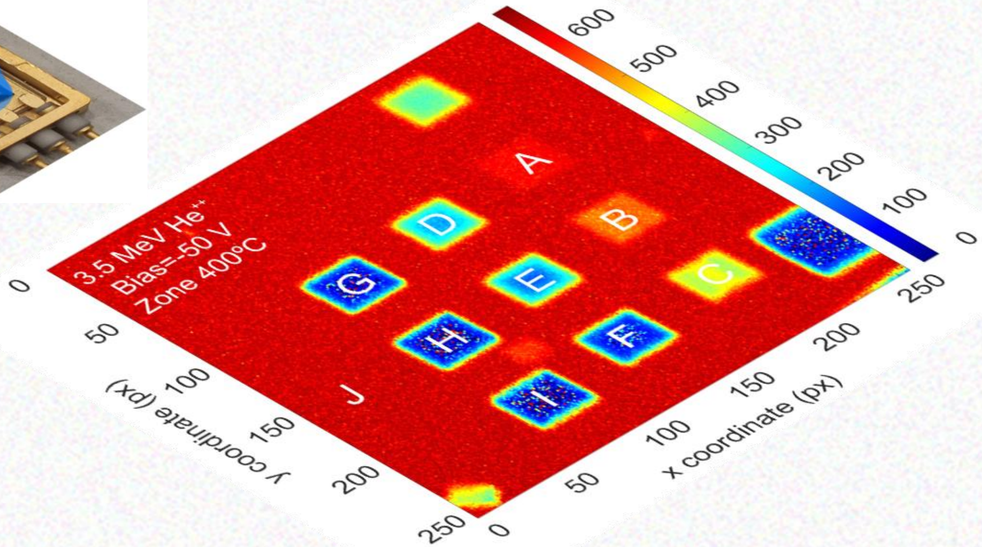

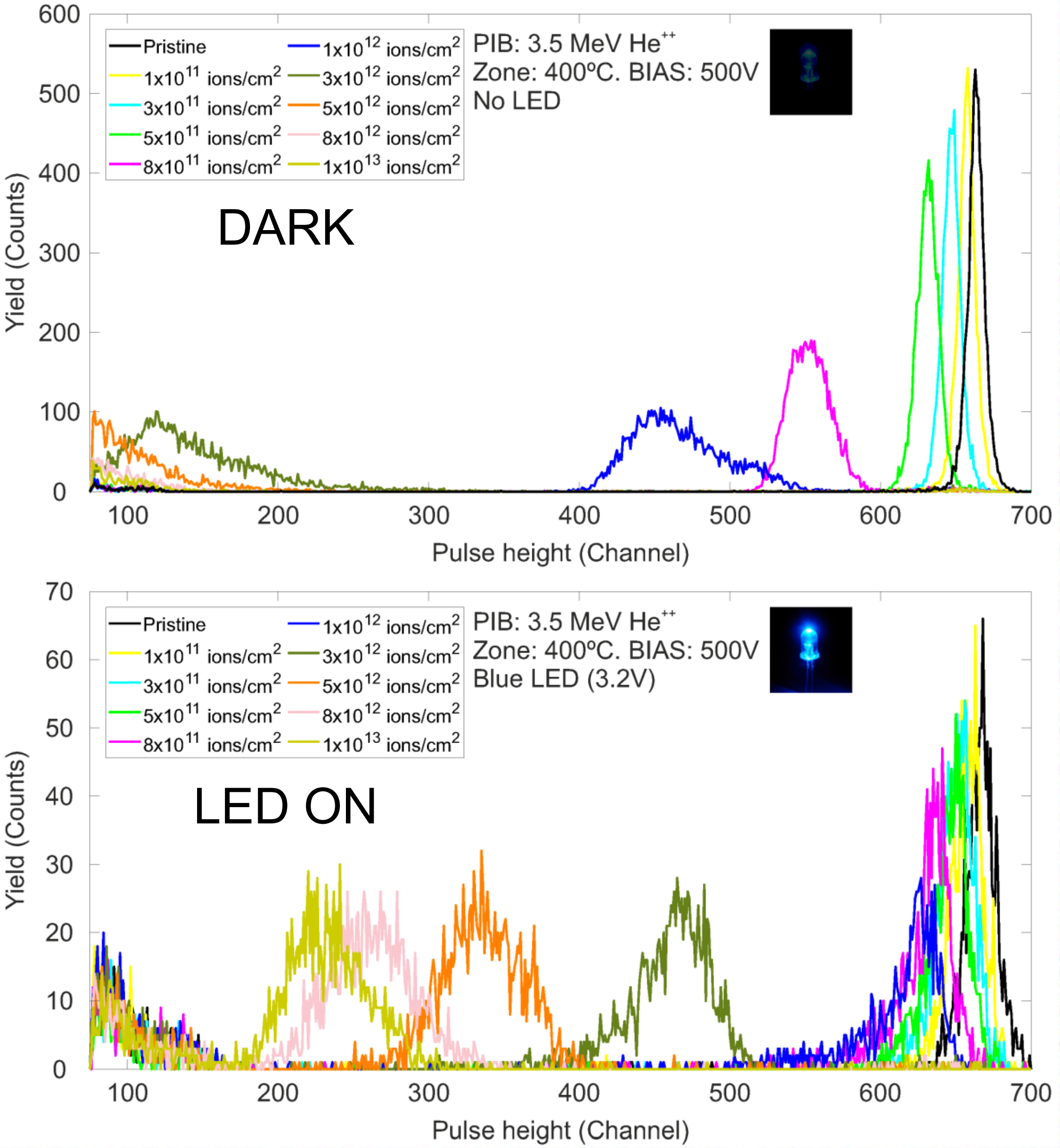

Rodríguez, M., et al. (2026). **Enhancing charge collection efficiency in radiation-damaged unmetallized 4H-SiC detectors via sub-bandgap LED illumination**. *Radiation Physics and Chemistry*. Submitted for publication.

ILLUMINATION HAS A SIGNIFICANT EFFECT IN THE MOST DAMAGED REGIONS

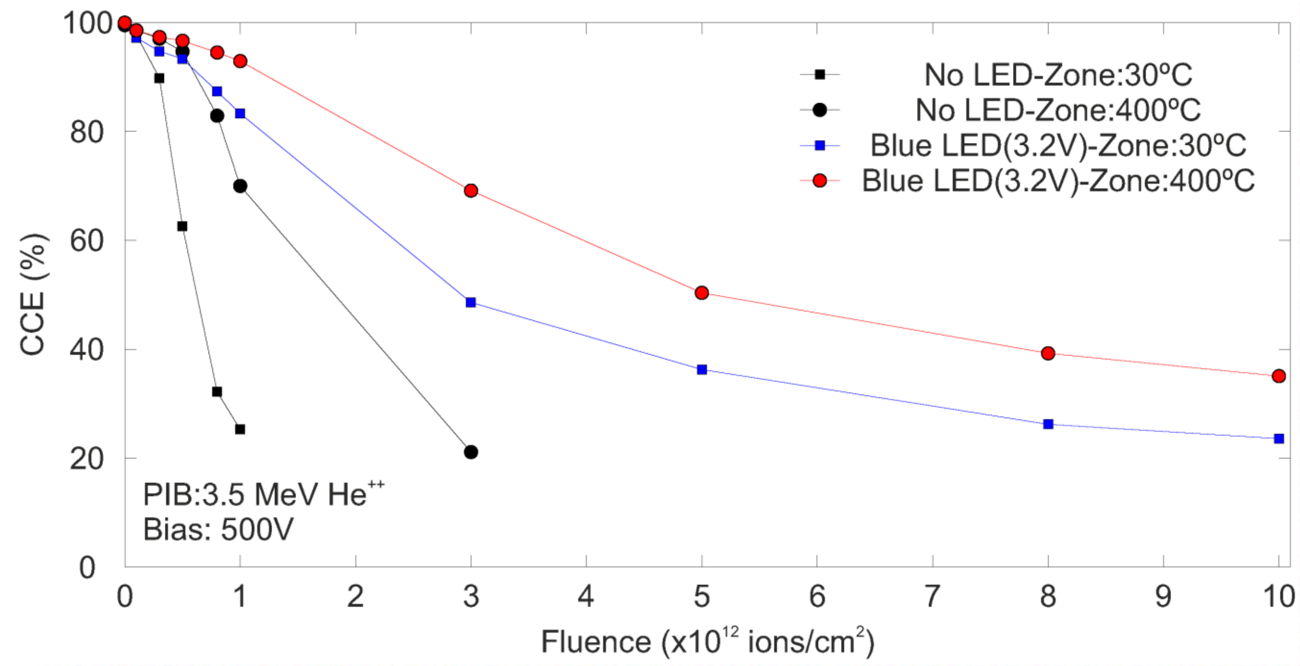

Photo-detrapping

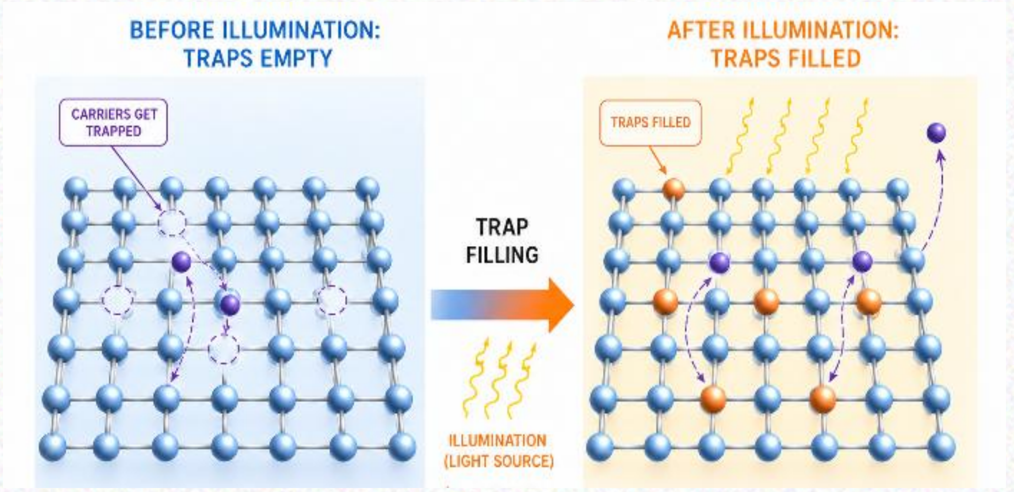

Trap filling

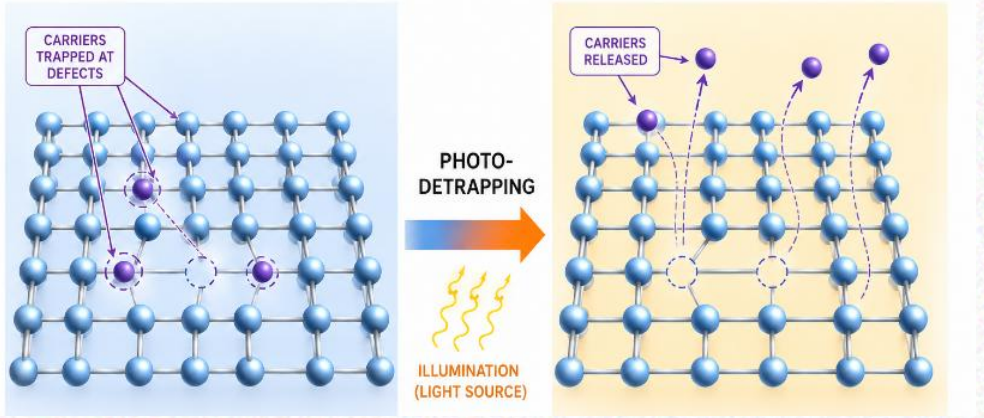

- Higher fluence drops the CCE, making damaged regions inaccessible.
- Illumination triggers photo-detrapping and trap-filling, which enhances the detector response.

Future work

High-Temperature SiC Measurements

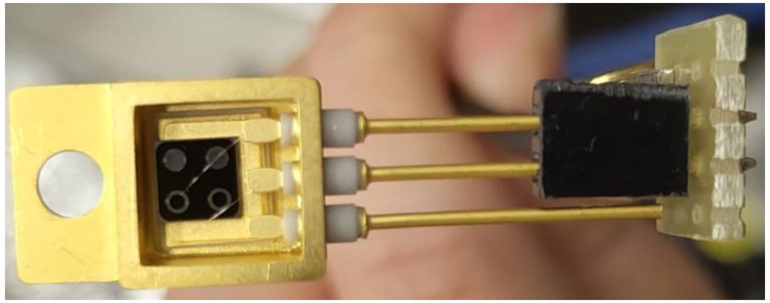

- **Graphene Contacts**: Evaluate a new detector architecture featuring surface graphene instead of metallic contacts.

- **In-Situ High-Temp Measurements**: Measure response directly at elevated temperatures, addressing furnace-induced noise challenges in the experimental setup.

- **Model Expansion & Kinetics**: Add an extra temperature point to refine MCMC parameter fitting and determine if graphene alters defect stabilization.

DRD3 WP3 Project: SiC-LGAD Detectors ???

Determination of the Relative Defect Density in Si using SPA-TCT and TPA-TCT Method

Different ion implantations in 4 silicon (300 μm) **PIN** diodes :

- ➢ 4 MeV H^{+}
- ➢ 12 MeV O^{5+}
- ➢ 20 MeV Si^{8+}
- ➢ 8.4 MeV N^{4+}

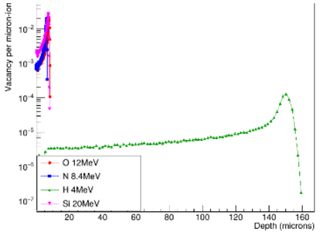

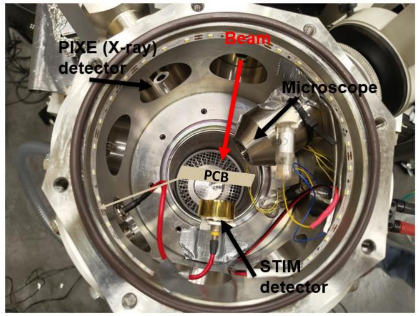

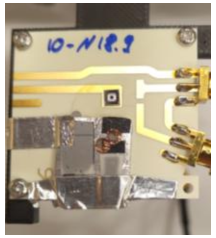

TCT: red laser (650nm = 1.9 eV)

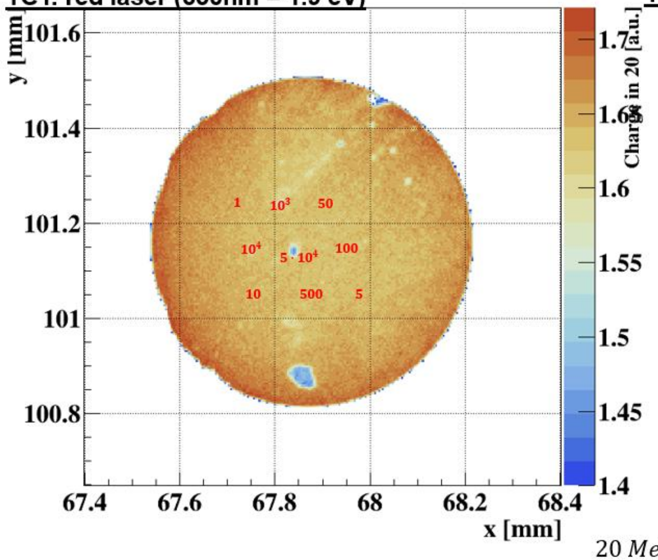

TPA-TCT: SWIR laser (1550nm = 0.8 eV)

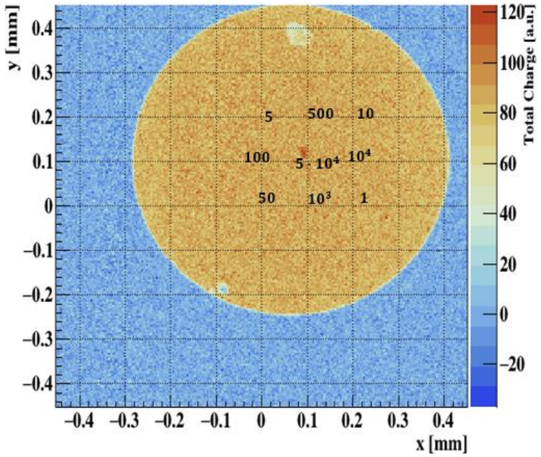

20 MeV Si^{8+}

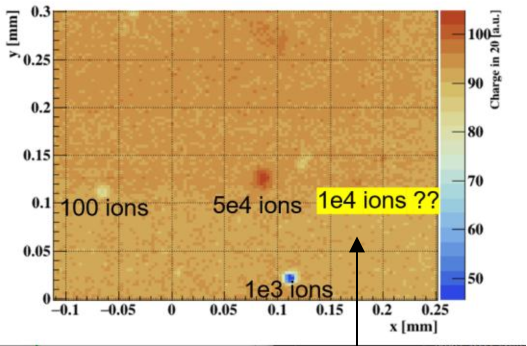

Position determing with TCT: red laser (650nm = 1.9 eV)

Spot size of ≈ 20 μm diameter and fluences ranging from 1 to 5×10^4 ions .

- Due to spot size → z-dependence on SPA contribution.
- TPA Threshold: High sensitivity, down to 100 ions (Si atoms)

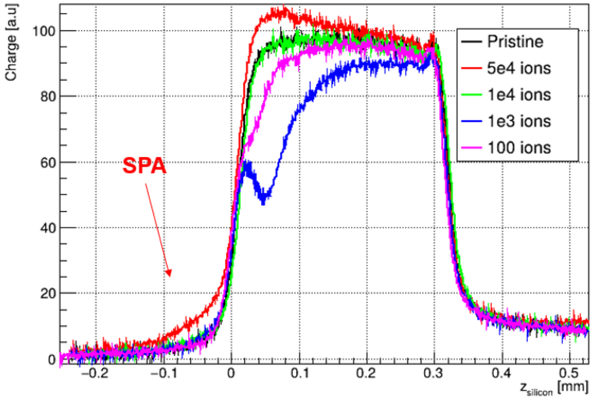

V = 160 V

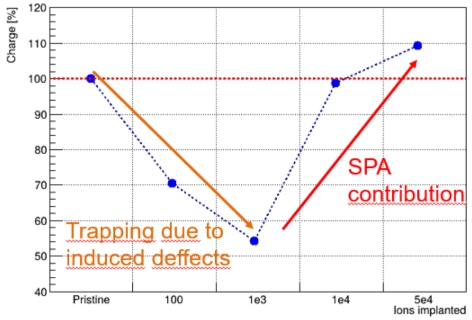

TPA-TCT shows **high 3D sensitivity**, revealing **charge loss and defect distribution** in silicon.

Future work

Defect Density Characterization

- IBIC Characterization: Perform Ion Beam Induced Charge (IBIC) measurements to compare against TPA-TCT and evaluate differences

- Larger Irradiation Areas: Irradiate larger spatial regions to eliminate **SPA-TCT z-dependence** artifacts arising from small-volume irradiation.

- Fluence Scan (100 to 10^5 ions): **Perform detailed steps around $\mathbf{10^3}$ ions** to investigate the charge minimum, where the response transitions from defect-trapping dominance to SPA contribution.

- Device Variability: Compare relative defect densities across **different thicknesses** (e.g., 300 μm vs. 50 μm) and manufacturers (e.g., CNM vs. Hamamatsu).

“Deep” CNM LGADs for CMS ETL (WP2.O1)

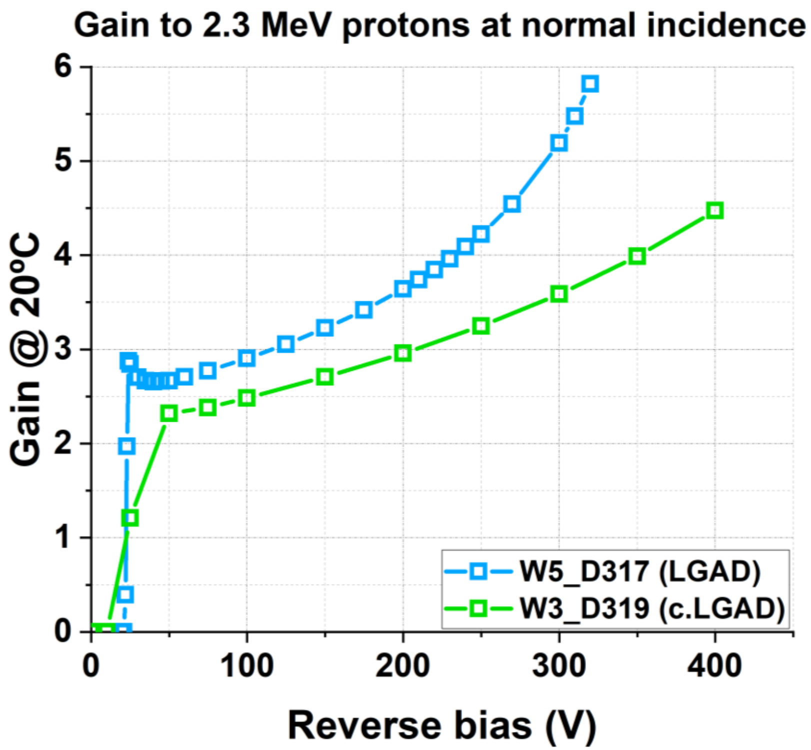

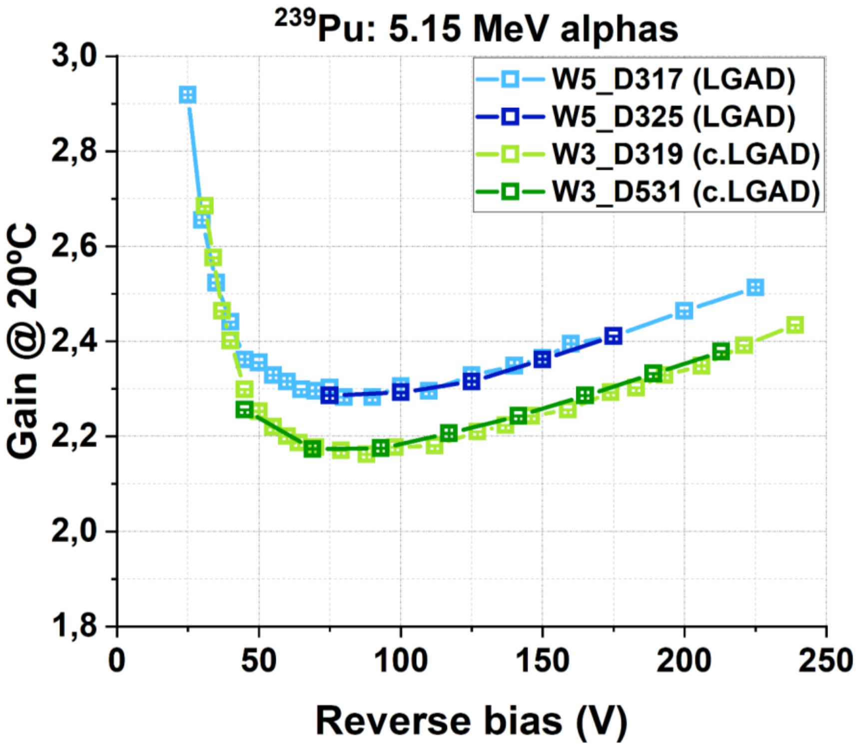

- CNM **Run17958** (“Deep” LGADs with arsenic implanted N++) → **Single pad diodes**
- Gain measurements at the microprobe beam line (protons of 2.3 MeV) and with a tri-Alpha source show that **carbonated “Deep” LGADs have a lower gain** when fabricated under the same conditions
- This effect is attributed to the distribution of carbon interstitials during boron difusión during fabrication
- **Fabrication Insight and gain measurements with trialpha source are published in Sensors Journal:** https://doi.org/10.3390/s25175571

“Deep” CNM LGADs for CMS ETL (WP2.O1)

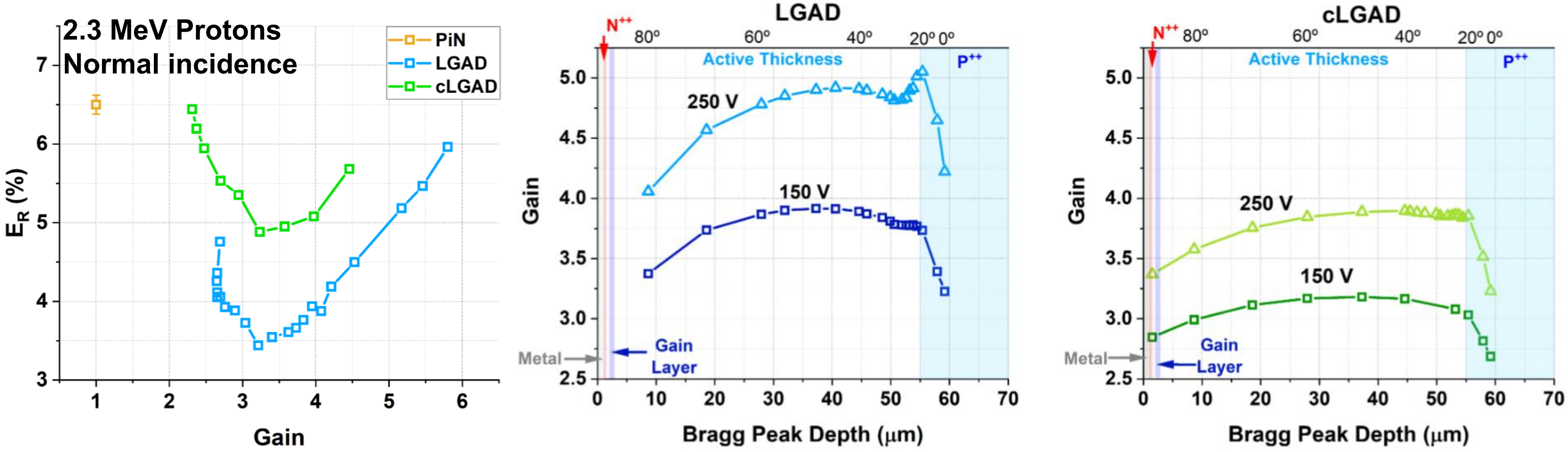

- For 2.3 MeV protons, **gain suppression** in both “Deep” LGAD and cLGADs **is not drastic** when varying the incidence angle (higher ionization density closer to PN junction as angle increases)
- Also, the **energy resolution at normal incidence is better for both “Deep” LGAD and cLGAD than for a standard PiN detector**
- These results are about to be published in IEEE Sensors Journal: **J. Villegas et al. Impact of Gain Suppression in LGADs on Energy Resolution for Charged Ion Spectrometry. IEEE Sensors Journal (2026),** ***Accepted for Publication in July 2026***
- Results were also presented at 4th DRD3 Workshop: https://indico.cern.ch/event/1581713/contributions/6759972/

TI-LGAD and CASSIA Detectors (WP3.O1)
DRD3 WP2 Project:TI-LGADs for 4D tracking and SiC-LGAD detectors.

Ongoing Collaboration (DRD3-WG2) with University of Zurich

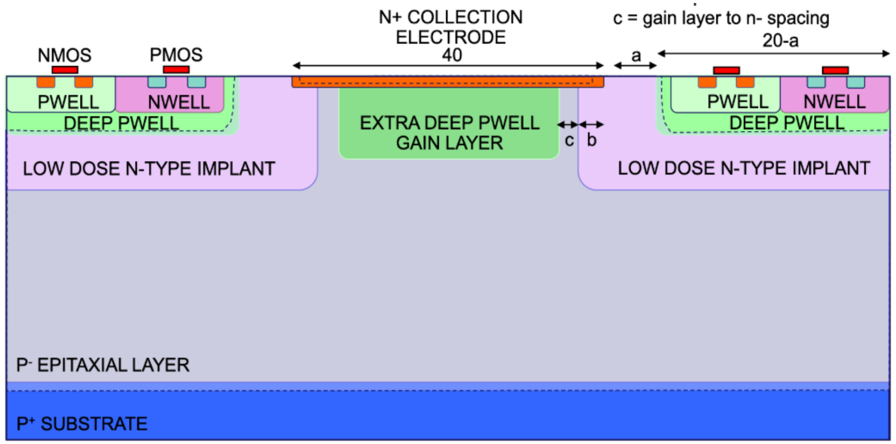

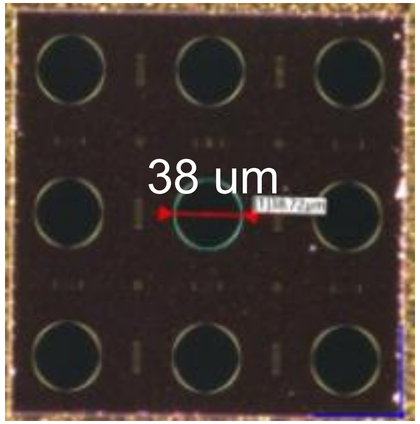

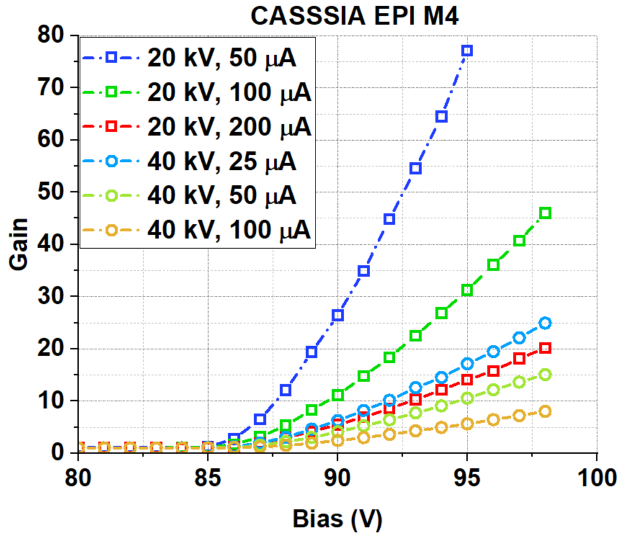

CASSIA → CMOS Pixelated LGAD detectors

- Gain measurements with x-ray tube
- **Strong gain suppression** observed when tuning x-ray intensity and max. Energy (20 and 40 keV)
- Results presented in 5th DRD3 Workshop: indico.cern.ch/event/1634258/contributions/7124301/
- IBIC measurements with protons are being analysed, showing no gain

TI-LGAD → 2x2 Pixelated LGADs

- IBIC measurements with 3 MeV protons are being analysed
- Preliminary results: a **gain of 3-4 is observed in the operational voltage** range (30-200 V)

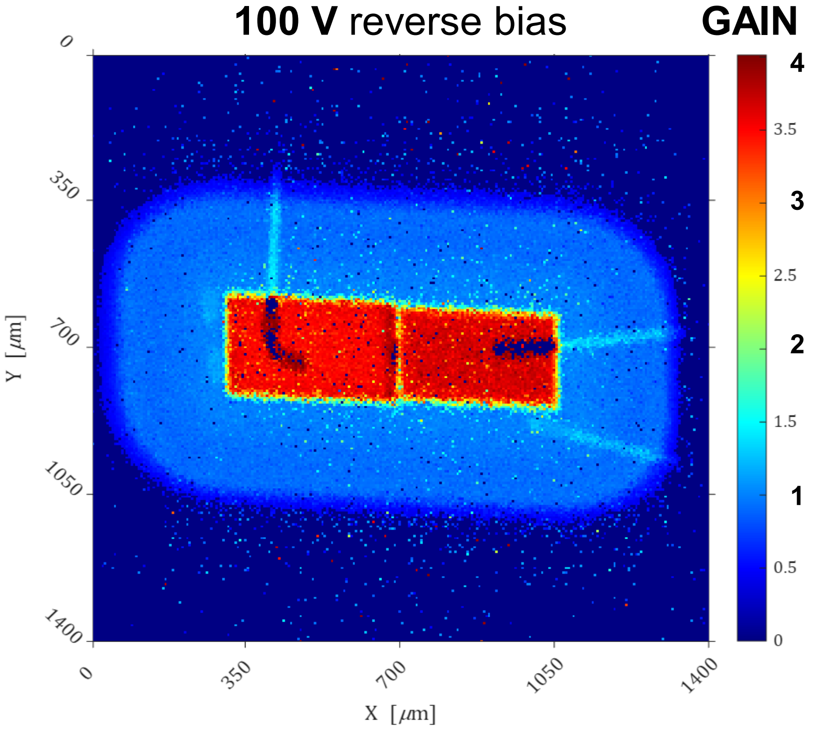

Wafer	Thickness	Carbon	Trench depth	Trench process
1	45	Y	D2	P2
2	45	Y	D2	P2
3	45	Y	D1	P2
4	45	Y	D1	P1
5	45	Y	D2	P1
6	45		D2	P2
7	45		D2	P2
8	45		D1	P1
9	55	Y	D3	P2
10	55	Y	D2	P2
11	55	Y	D2	P2
12	55		D2	P2

Wafer 5: V1-1TR-TW5

Wafer 9: V1-1TR-TW5 / V2-1TR-TW5 / V1-1TR-TW4 / V2-1TR-TW1 / V2-1TR-TW3

Wafer 11: V1-1TR-TW5 / V2-1TR-TW5

Wafer 12: V1-1TR-TW5 / V2-1TR-TW5

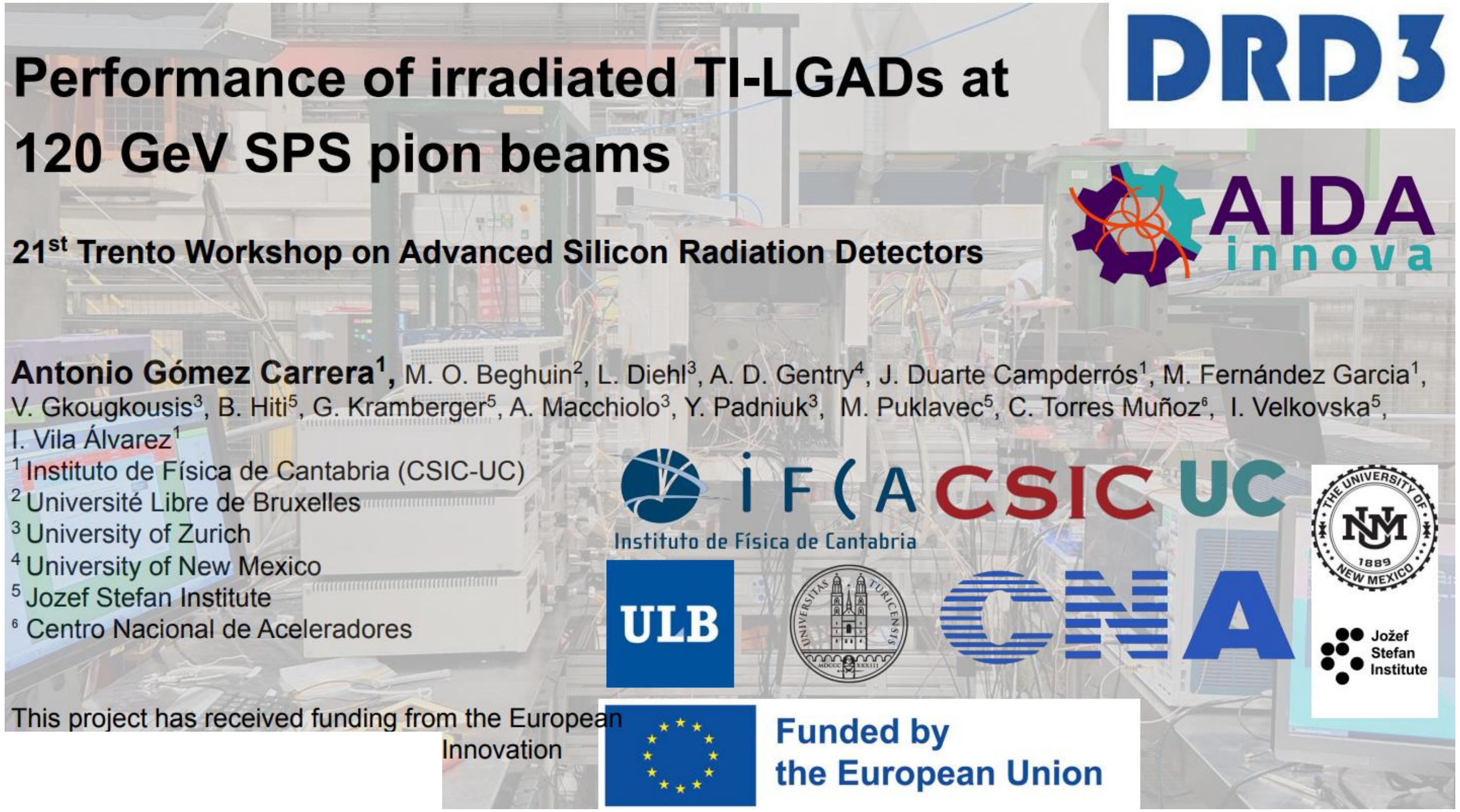

PREPARED FOR SUBMISSION TO JINST

Tracking and timing measurements on irradiated TI-LGADs

A. Gomez-Carrera[1 a] L. Diehl[b] J. Duarte-Campderros[a] M. Fernandez[a] V. Gkougkousis[b] B. Hiti[c] G. Kramberger[c] A. Macchiolo[b] Y. Padniuk[b] M. Puklavec[c] C. Torres Muñoz[d] I. Velkovska[c] I. Vila[a]

CNM Run18399 – 300 um thick LGADs for low penetrating particle detection (WP3.O1)

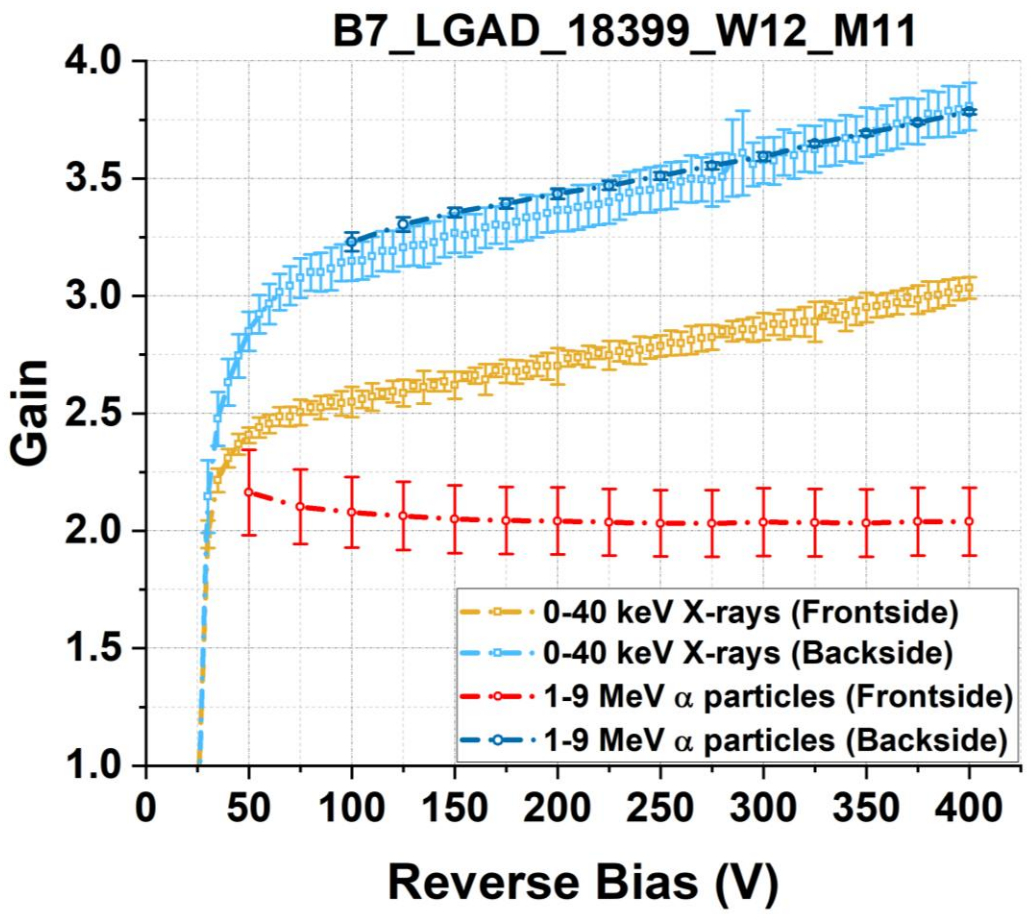

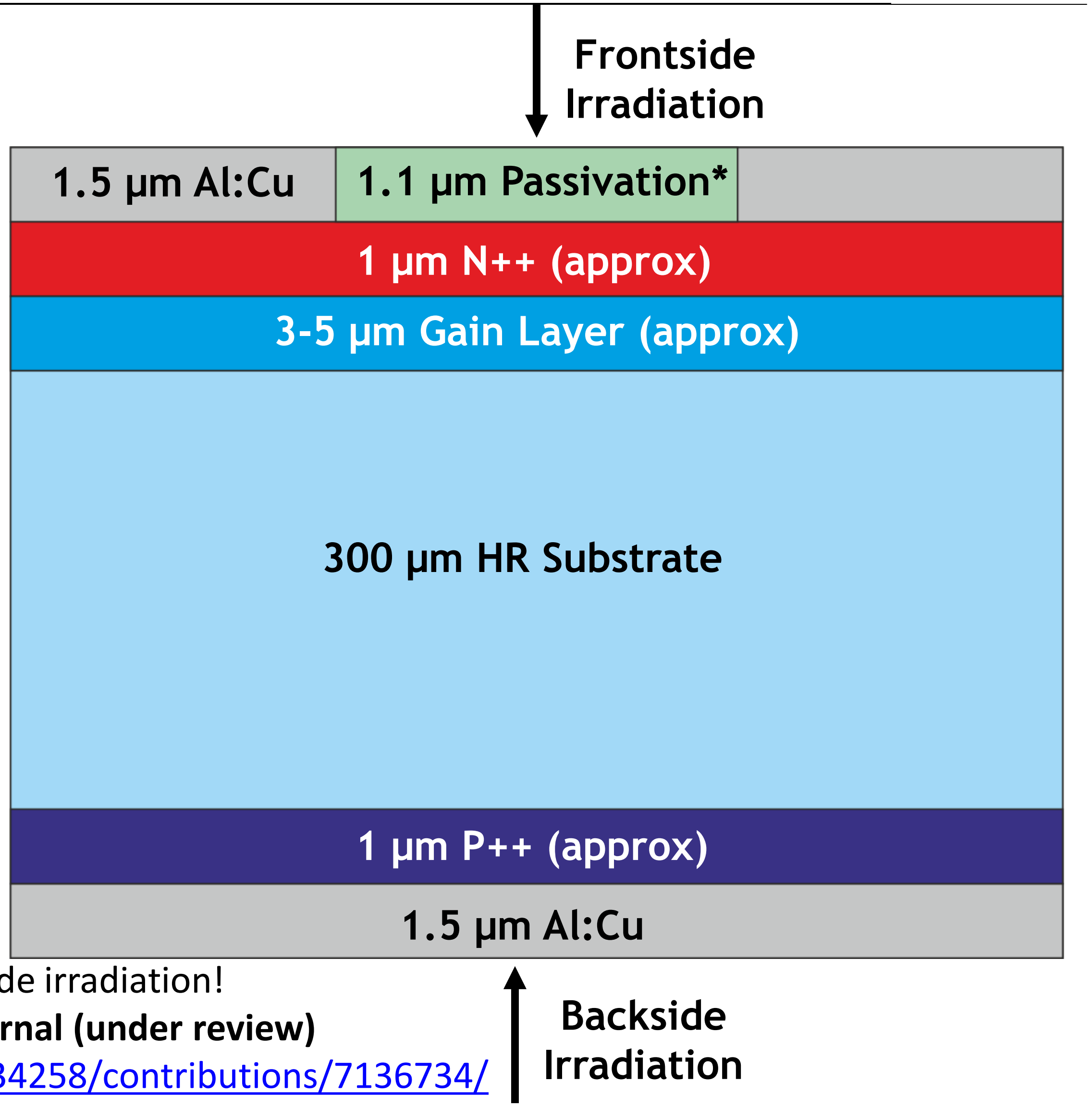

- **No Gain suppression observed** between x-rays and Alpha particles for backside irradiation!
- **Alpha particle results are submitted to Radiation Physics and Chemistry Journal (under review)**
- Results were also presented at 5th DRD3 workshop: indico.cern.ch/event/1634258/contributions/7136734/

Future work on LGADs

Centro Nacional de Aceleradores
INFRAESTRUCTURAS CIENTÍFICAS Y TÉCNICAS SINGULARES
UNIVERSIDAD DE SEVILLA

LGADs for CMS ETL

- IBIC Measurements on 2x2 pixelated devices to study gain uniformity and pixel isolation structures
- Gain measurements with x-rays

TI-LGAD Collaboration

- IBIC Measurements with LGADs of different configurations (different gain, trench width, trench number, carbon co-implantation, etc)

LGAD for low-penetrating particles

- nLGAD → New run finished at CNM: Alpha spectrometry, IBIC and x-ray measurements
- 300 um thick LGADs → Measurements of lenvironmental samples (heavy ion detection)

Characterization of ultra-thin (3 um) 4H-SiC diodes (WP3.O2)

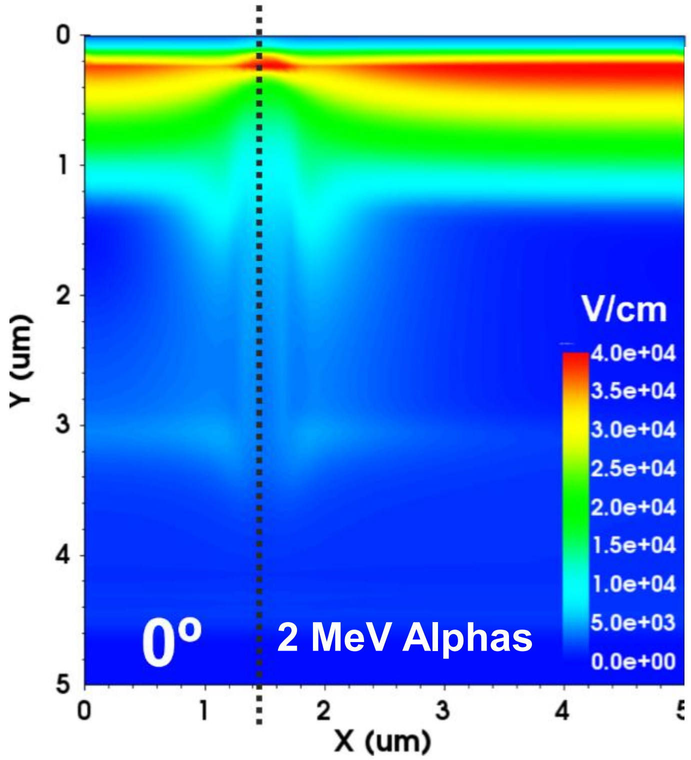

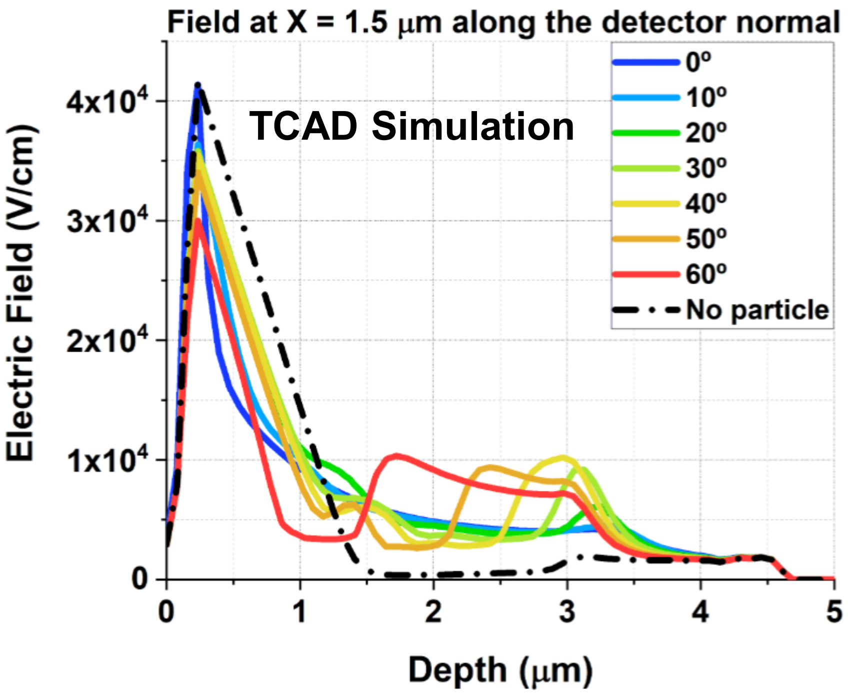

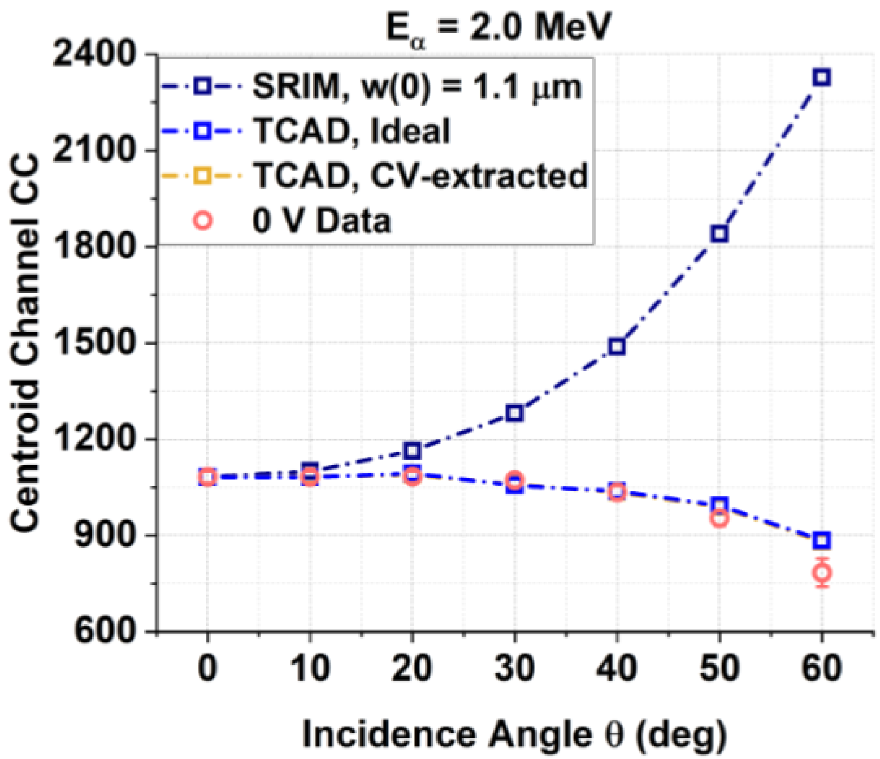

- **Funneling effects** is present in non-polarized ultra-thin 4H-SiC detectors during alpha particle detection → **The electric field gets distorted when a highly ionizing charged particle is traversing a semiconductor, transiently enhancing charge collection**
- Results were presented at 5th DRD3 workshop: indico.cern.ch/event/1634258/contributions/7138855/
- **Also, the results were submitted to Radiation Physics and Chemistry Journal (under review)**

Characterization of ultra-thin (3 um) 4H-SiC diodes (WP3.O2)

Centro Nacional de Aceleradores
INFRAESTRUCTURAS CIENTÍFICAS Y TÉCNICAS SINGULARES

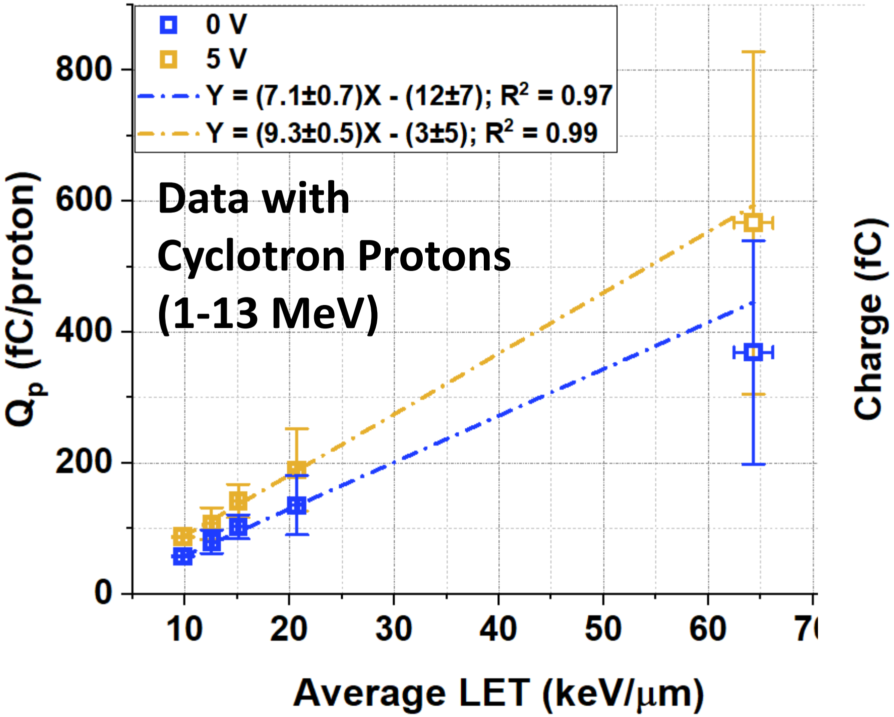

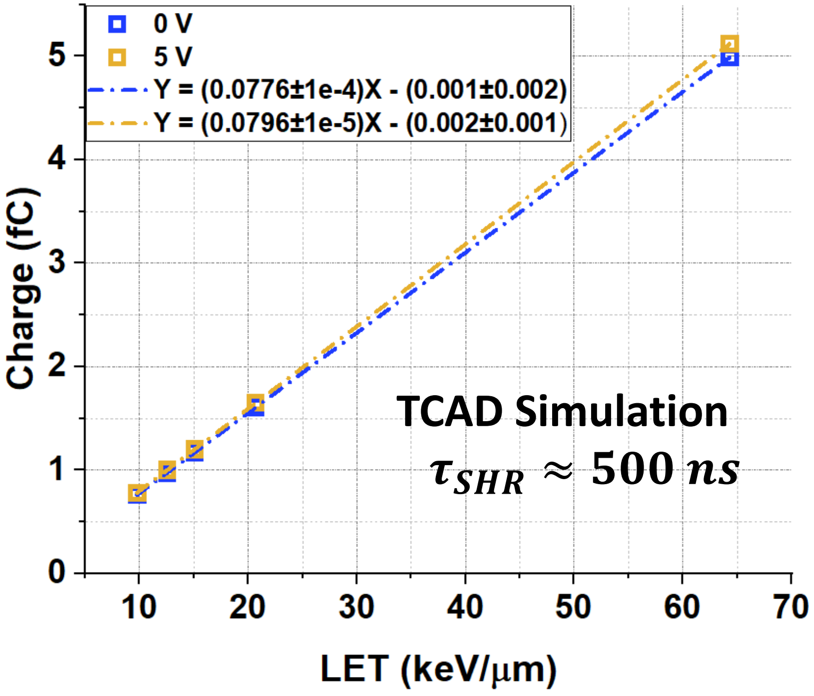

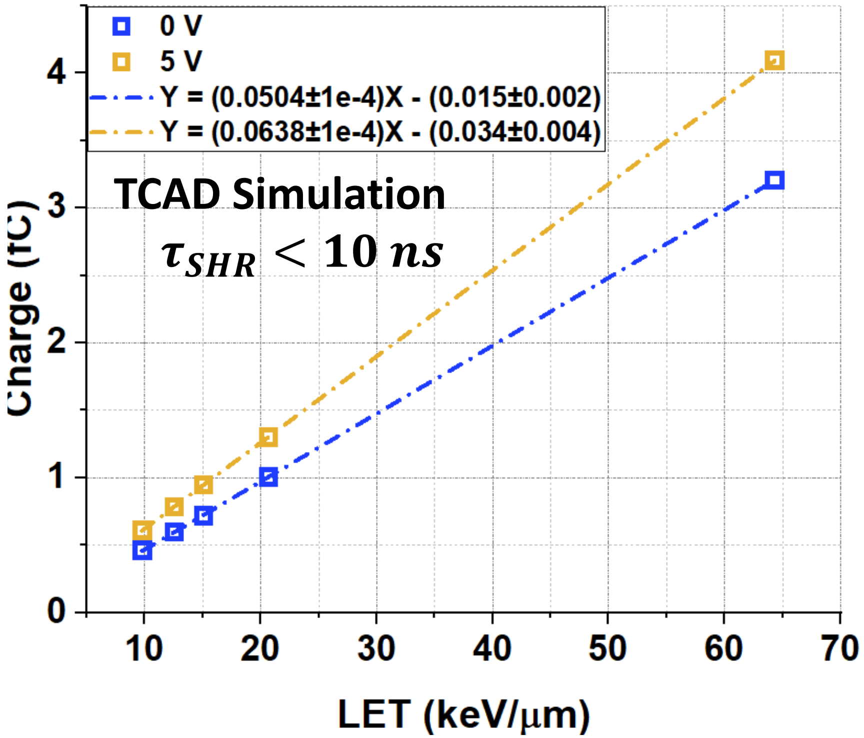

- **Measurements with Cyclotron Protons** (1-13 MeV → LET of 10-65 keV/um) are carried out and compared to TCAD simulations
- $\frac{Q_p(5V)}{Q_p(0V)}(Sim; \tau_{SHR} < 10ns) = 1.27$; $\frac{Q(5V)}{Q(0V)}(Data) = 1.30$ → **Similar change ratio between 0 and 5 V (both under full depletion) is observed in Simulation and Data when the SHR recombination time in simulation is adjusted**
- Potential to **develop a technique for indirectly measuring the SRH recombination lifetime** (associated with lattice defects before and after irradiation) in silicon and SiC detectors → Combination of alpha/proton measurements at low bias voltage and TCAD simulations

Future work on ultra-thin 3 um SiC diodes

Centro Nacional de Aceleradores
INFRAESTRUCTURAS CIENTÍFICAS Y TÉCNICAS SINGULARES
UNIVERSIDAD DE SEVILLA

Ultra-thin 3 um SiC diodes

- Measurements at the Cyclotron Line (Protons of 18 MeV) → Beam timing shape measurements with SiC diode and fibres detector

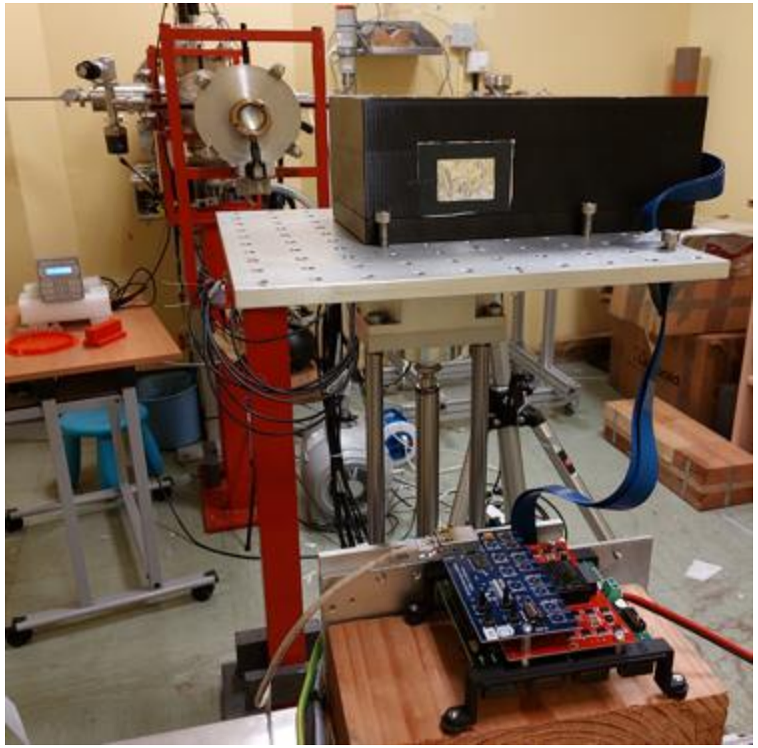

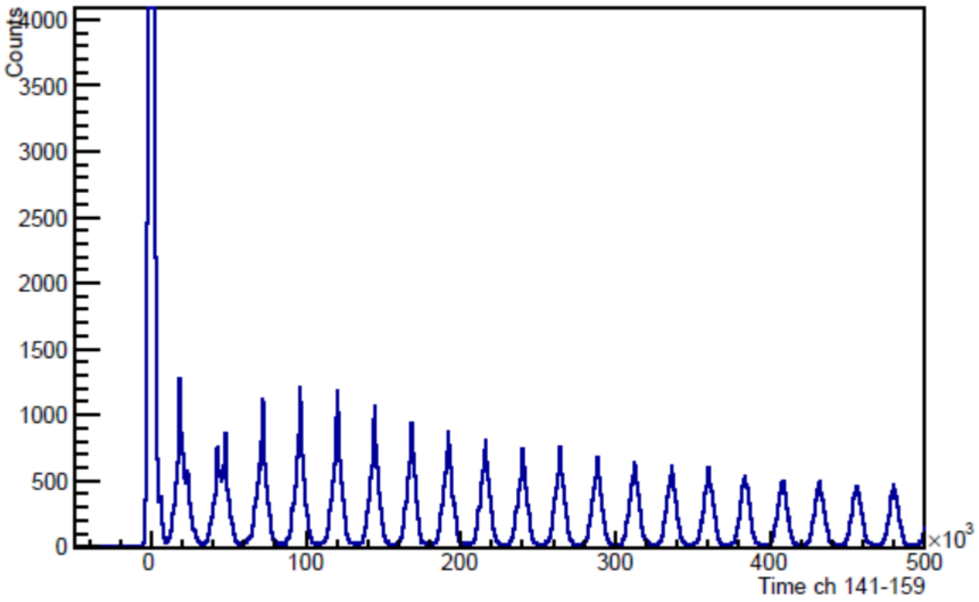

CHARACTERIZATON OF 3D DETECTORS WITH HEXAGONAL PIXEL CELL (WP3.O2)

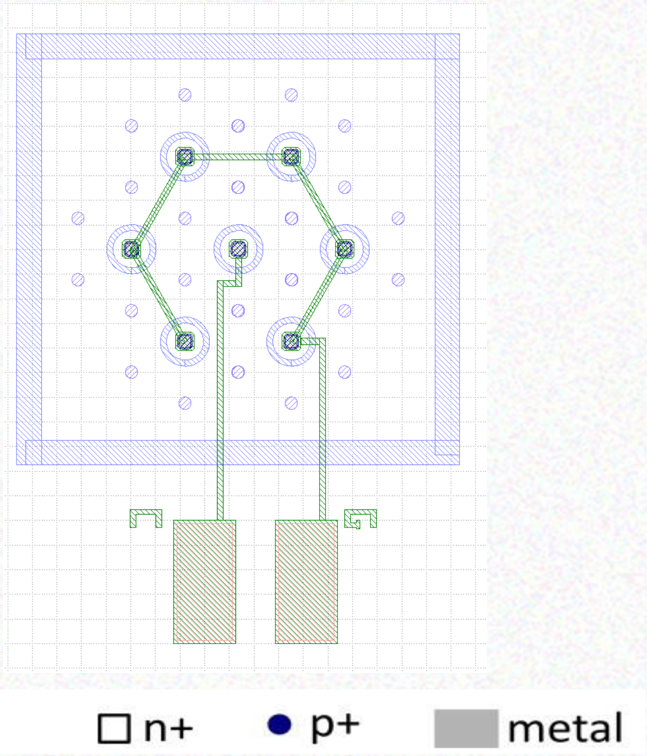

Central n-type electrode

Outer p-type electrodes

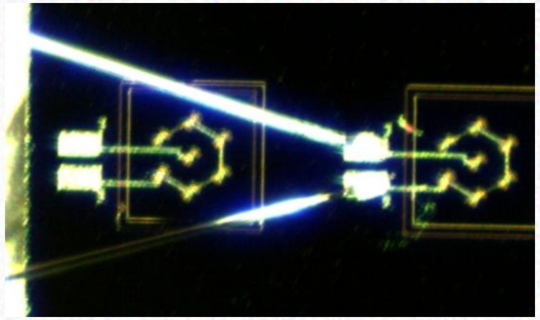

- 3D pixel sensors are being considered for timing at extreme radiation environments.
- Unirradiated double-sided 3D columnar-electrode sensors with a hexagonal pixel cell layout manufactured at IMB-CNM.
- Central pixel cell is readout and the neighbouring cells are shorted to the ground.
- The distance between n+ and p+ columns is 50 μm.

CHARACTERIZATION AT THE CNA ION BEAM NUCLEAR MICROPROBE

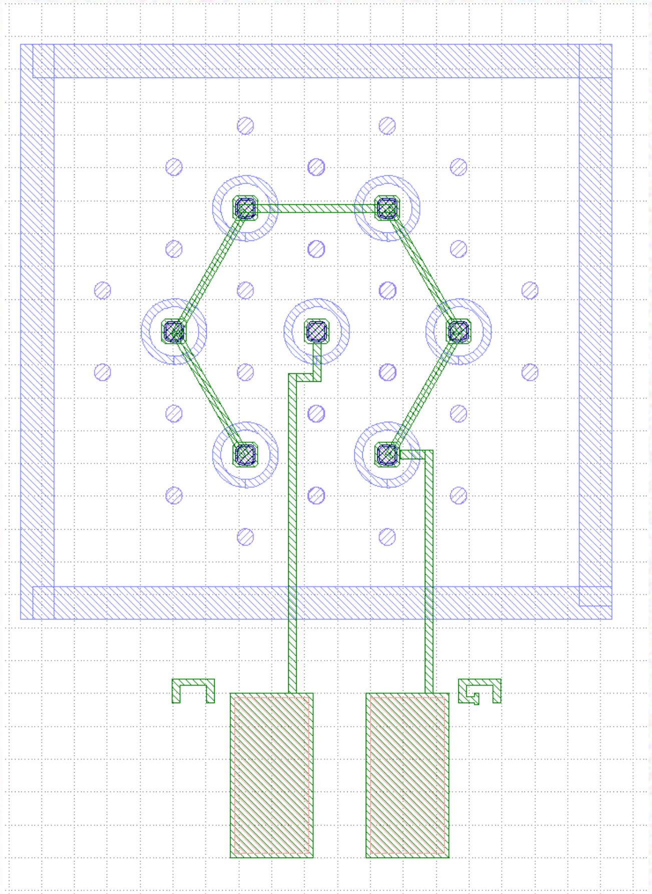

- IBIC and TRIBIC characterization using a 4 MeV H^+ beam (range approximately 150 μm) with an average rate of 600 Hz and a spatial resolution of < 5 μm.

CHARACTERIZATION AT THE CNA ION BEAM NUCLEAR MICROPROBE

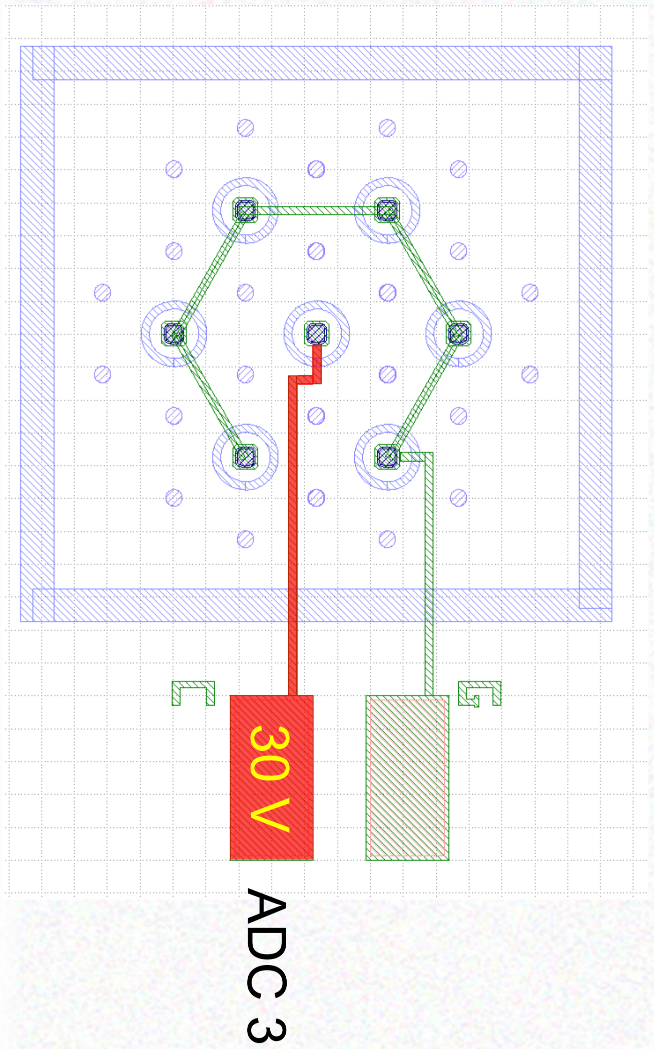

- IBIC and TRIBIC characterization using a 4 MeV H^+ beam (range approximately 150 μm) with an average rate of 600 Hz and a spatial resolution of < 5 μm.
- The **central** and peripheral electrodes (n^+ cylinders) were biased using different combinations of applied voltage, and the resulting induced currents were recorded.

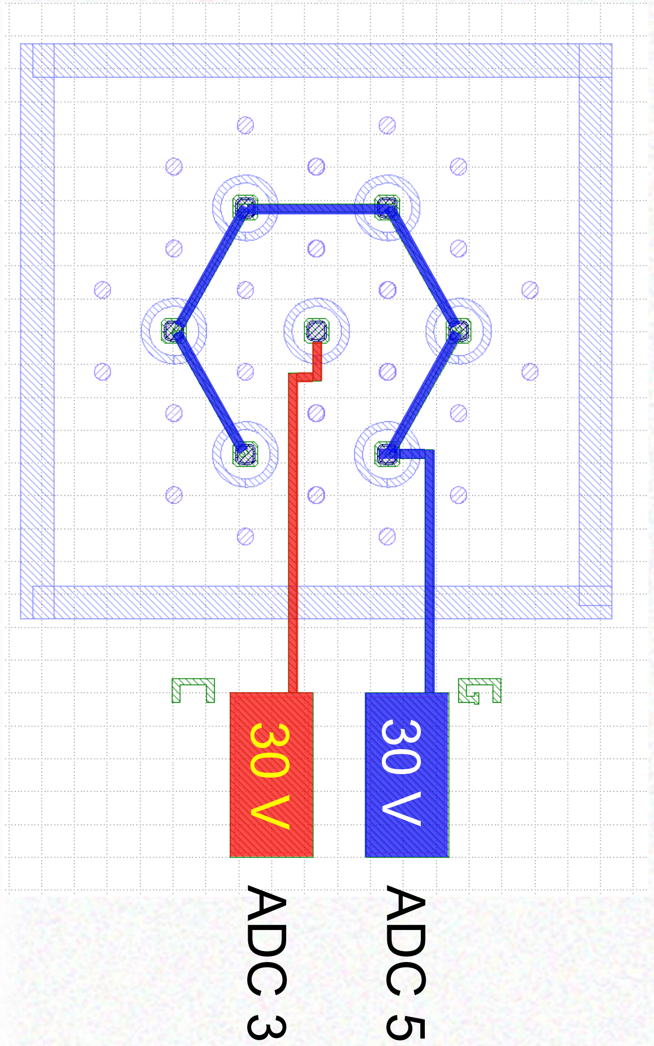

- IBIC and TRIBIC characterization using a 4 MeV H^+ beam (range approximately 150 μm) with an average rate of 600 Hz and a spatial resolution of < 5 μm.

- The central and **peripheral** electrodes (n^+ cylinders) were biased using different combinations of applied voltage, and the resulting induced currents were recorded.

Preliminary analysis

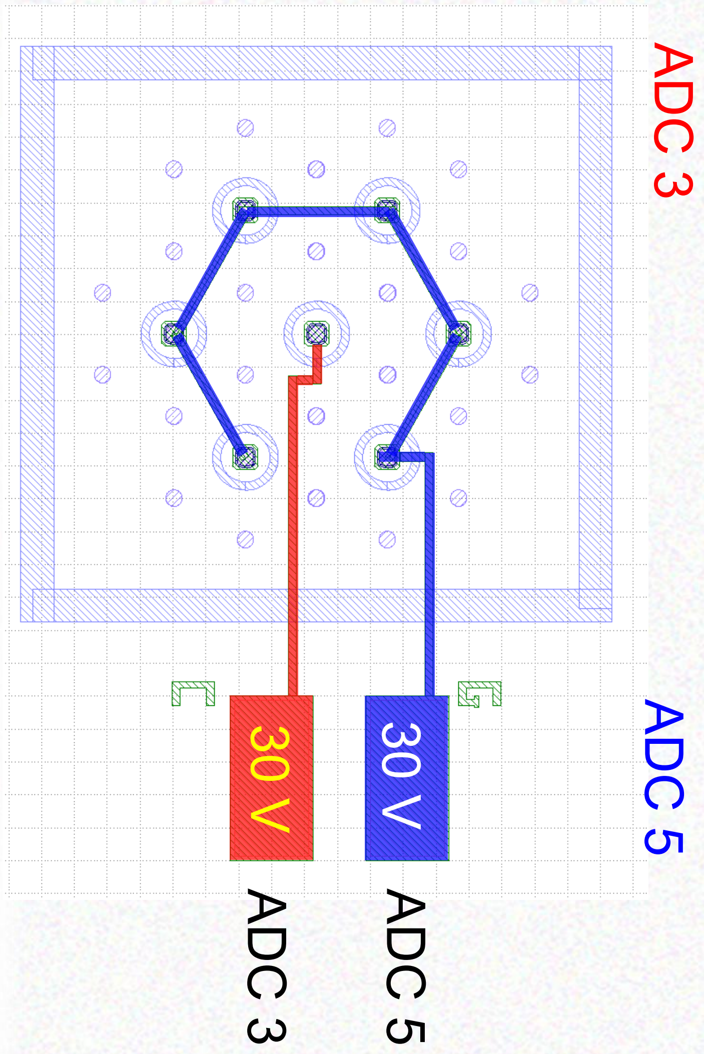

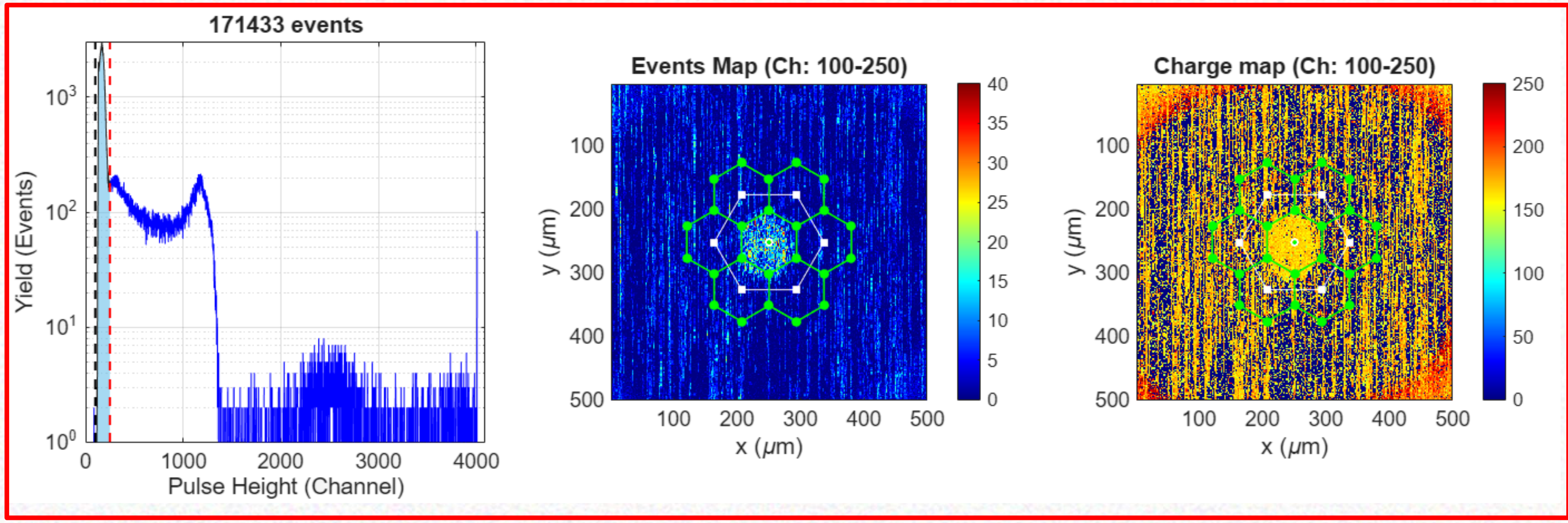

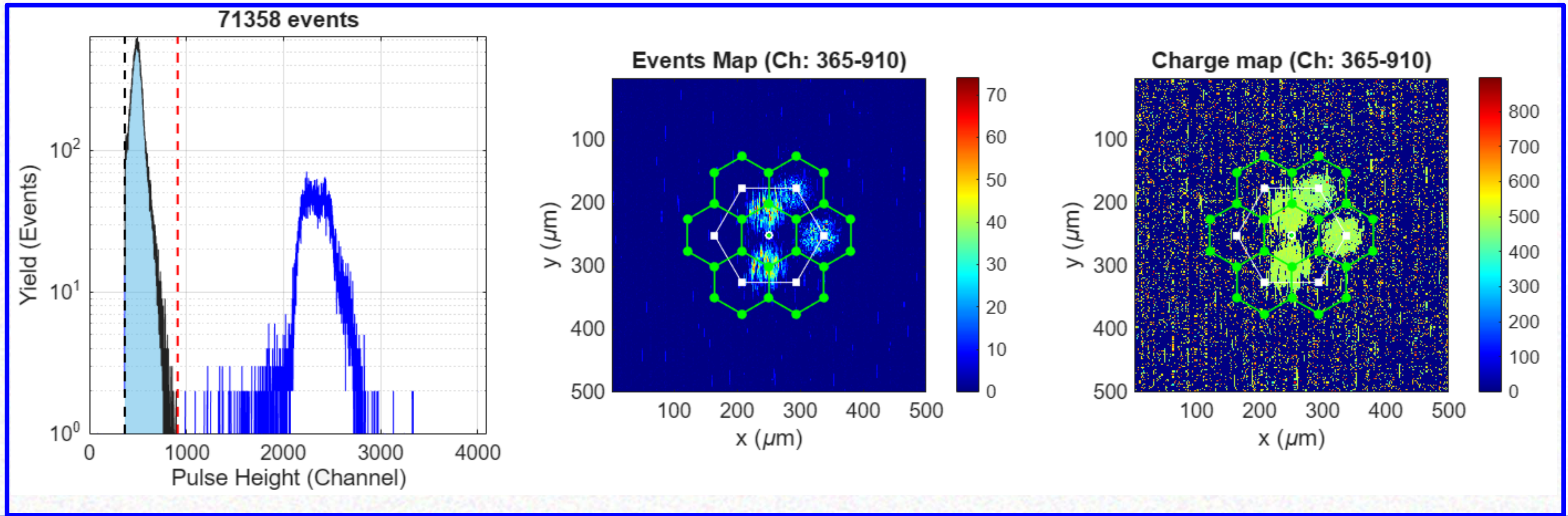

CHARACTERIZATION AT THE CNA ION BEAM NUCLEAR MICROPROBE

Preliminary analysis

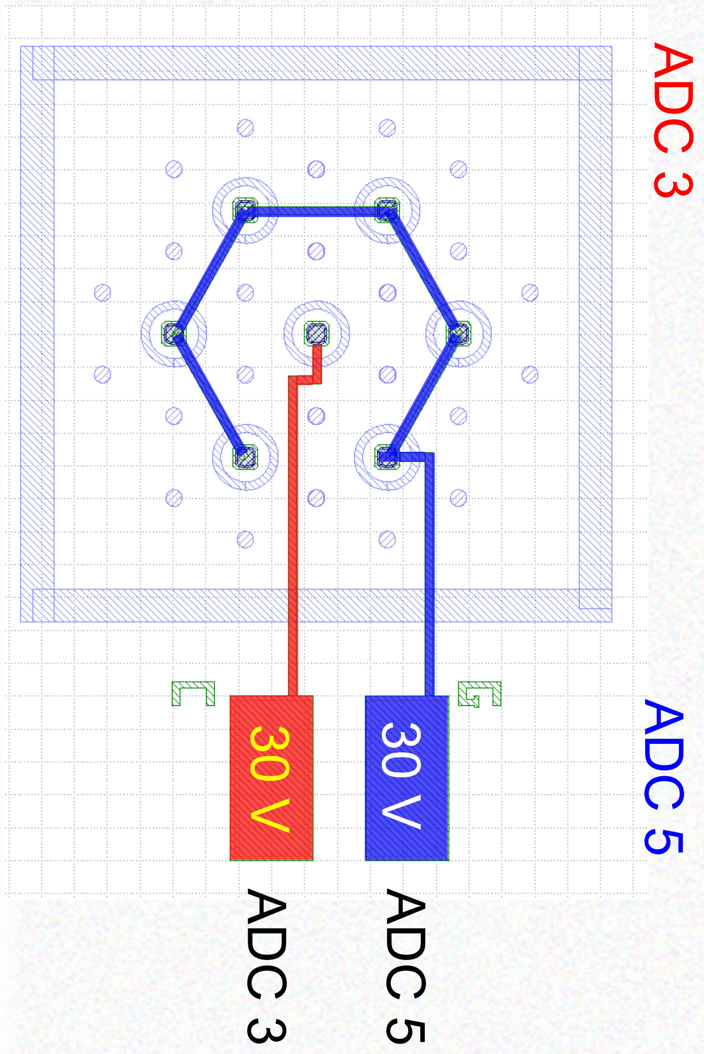

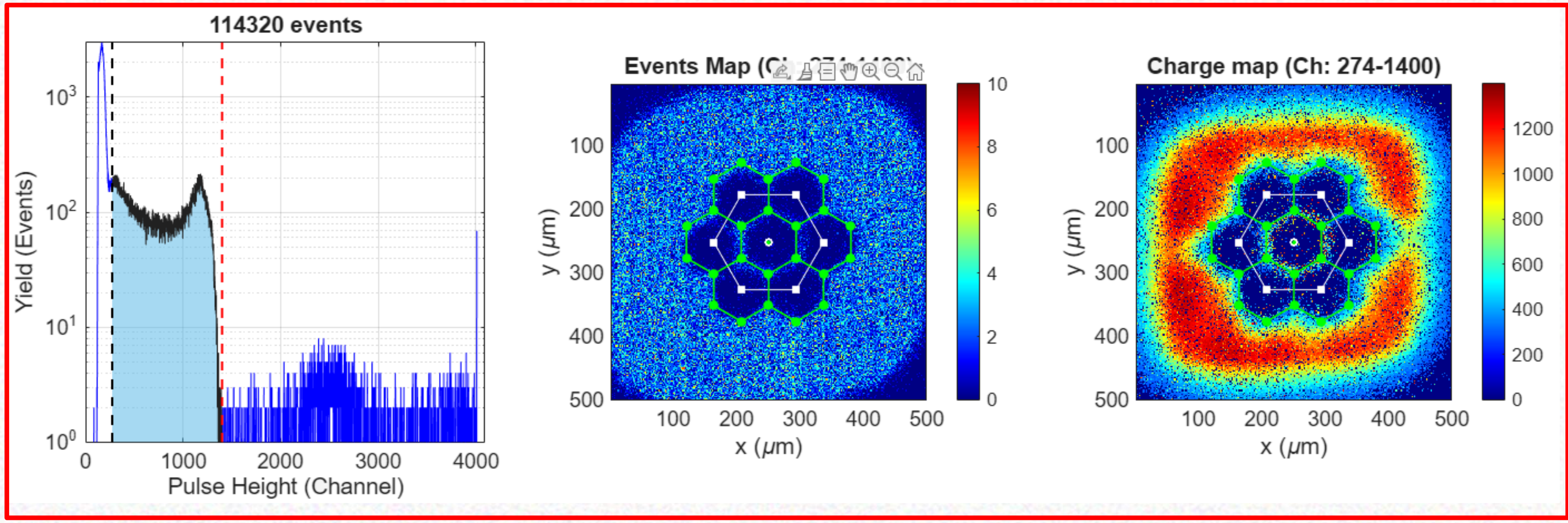

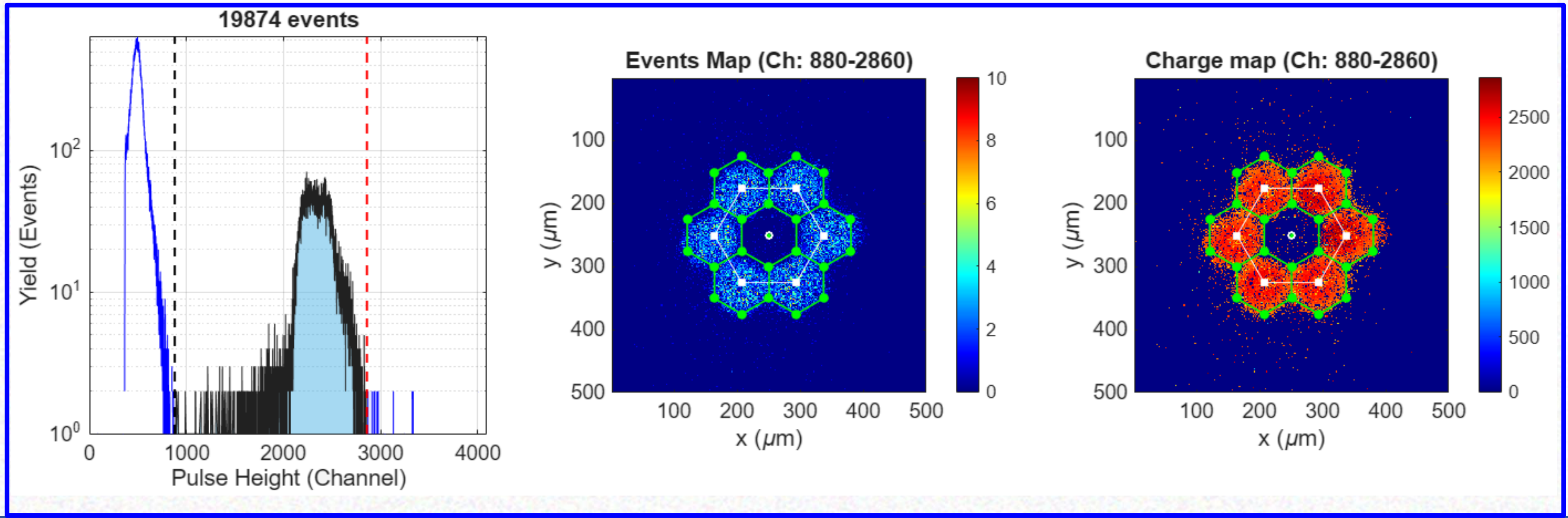

CHARACTERIZATION AT THE CNA ION BEAM NUCLEAR MICROPROBE

Preliminary analysis

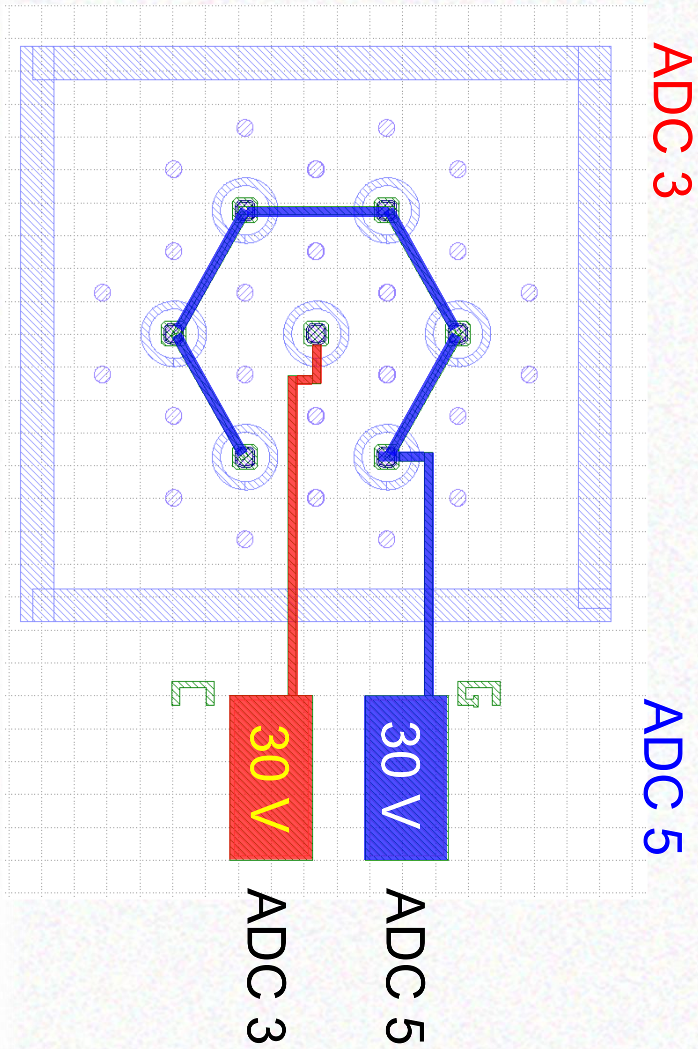

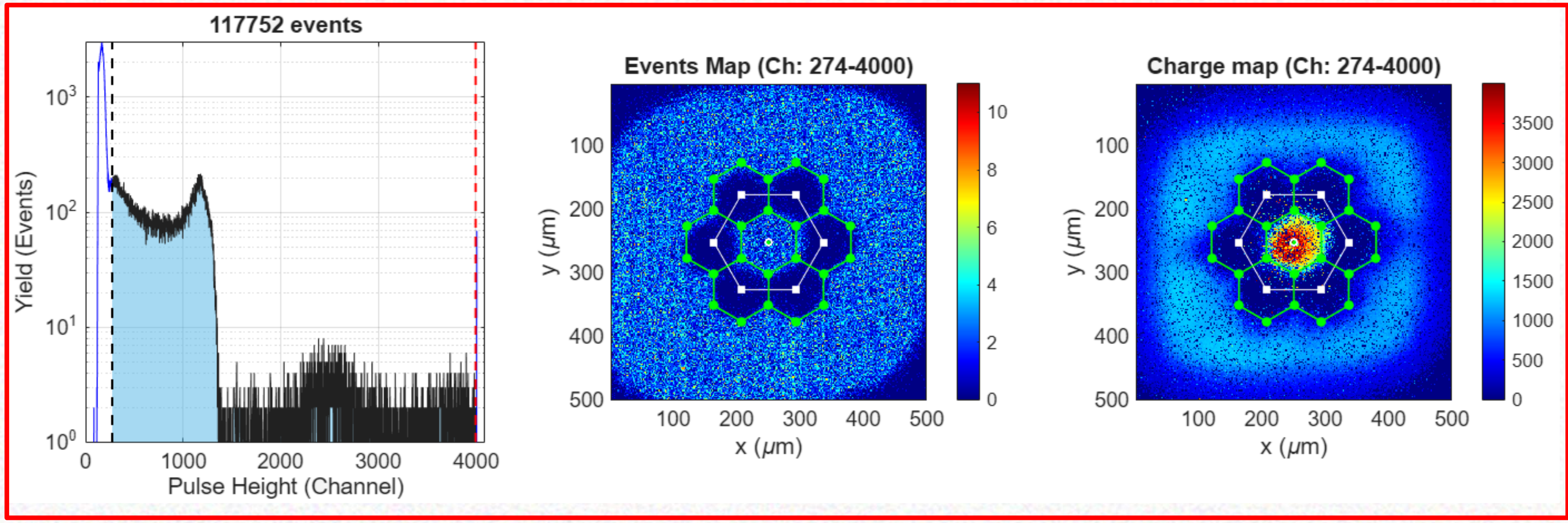

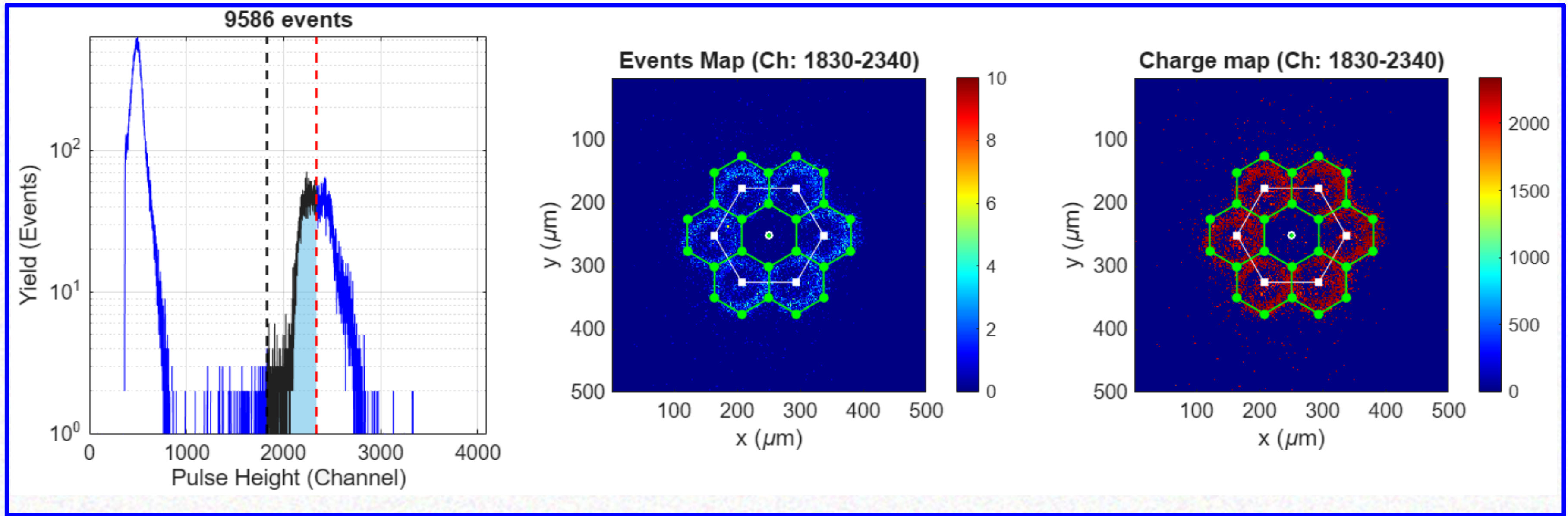

CHARACTERIZATION AT THE CNA ION BEAM NUCLEAR MICROPROBE

Preliminary analysis

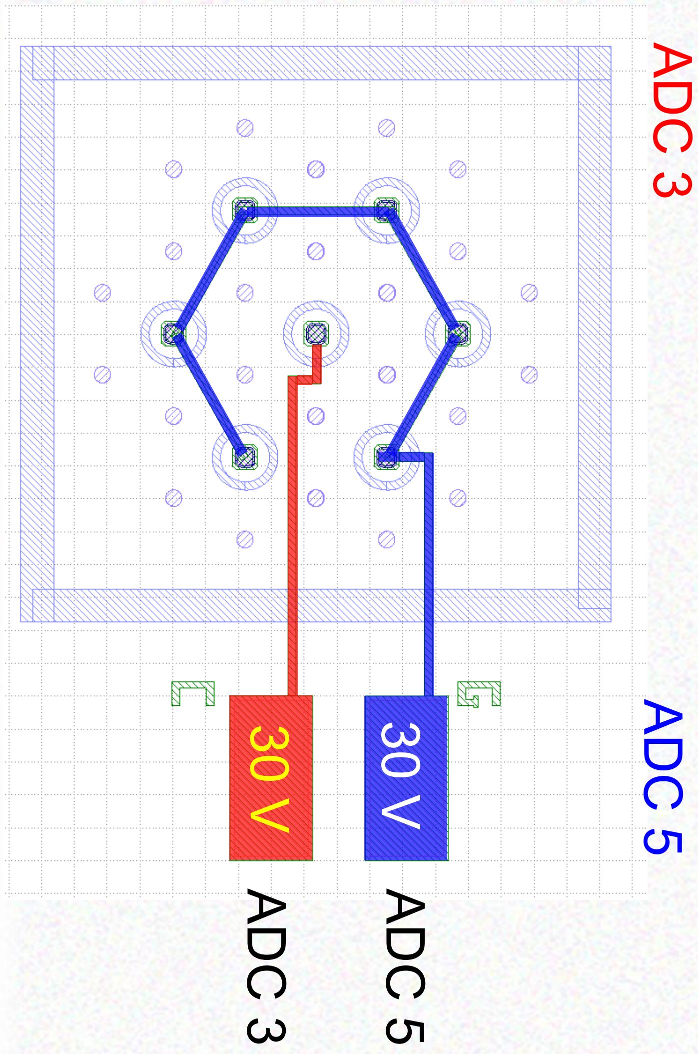

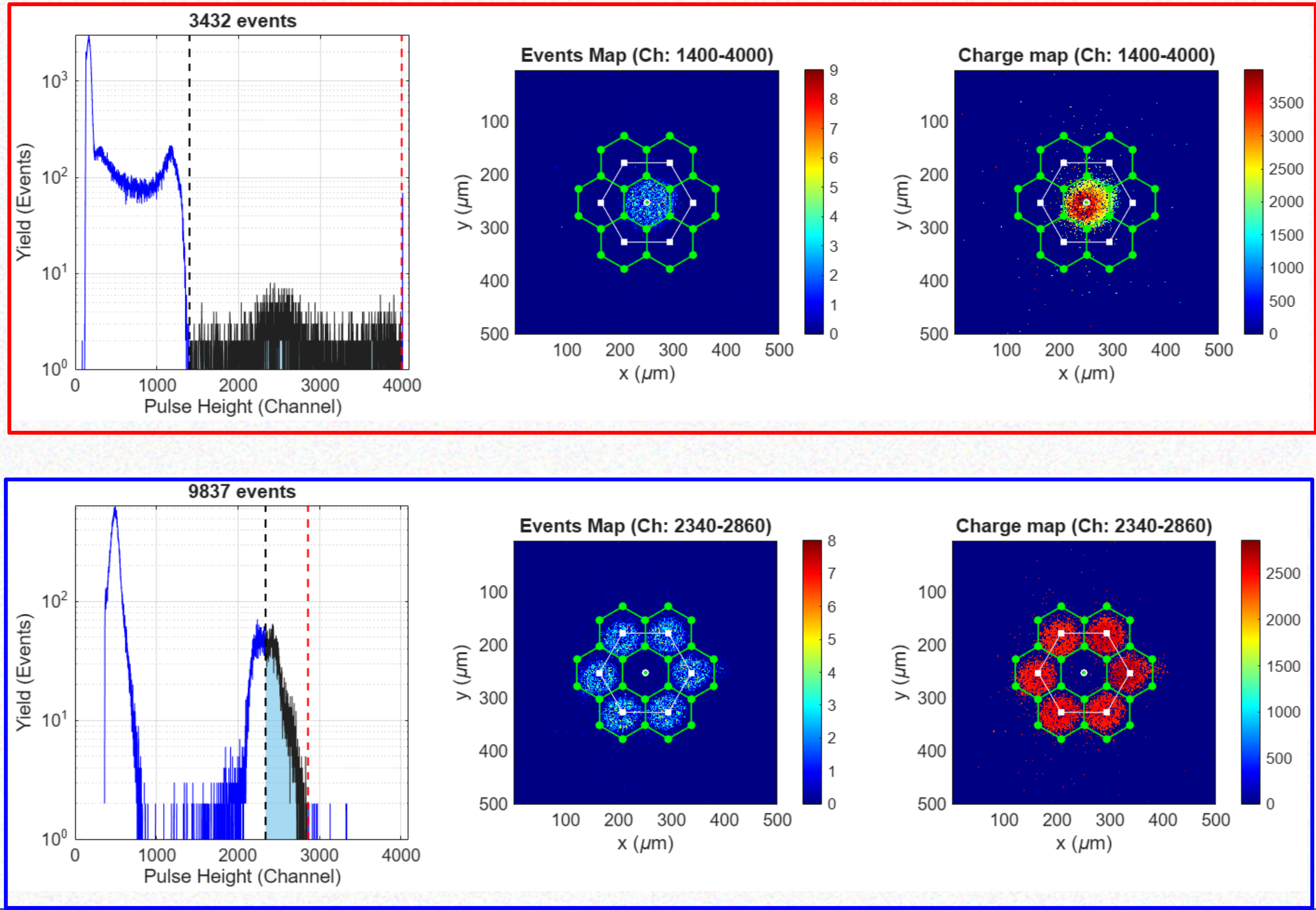

IBIC MEASUREMENTS ARE CURRENTLY UNDERWAY

- Apparently, the charge induced in each electrode comes only from the hexagonal pattern region surrounding each electrode.

- The detector's characterization is currently under analysis, focusing on identifying spatial patterns.

- **Future Work**: Conducting energy scans using calibrated ADCs.

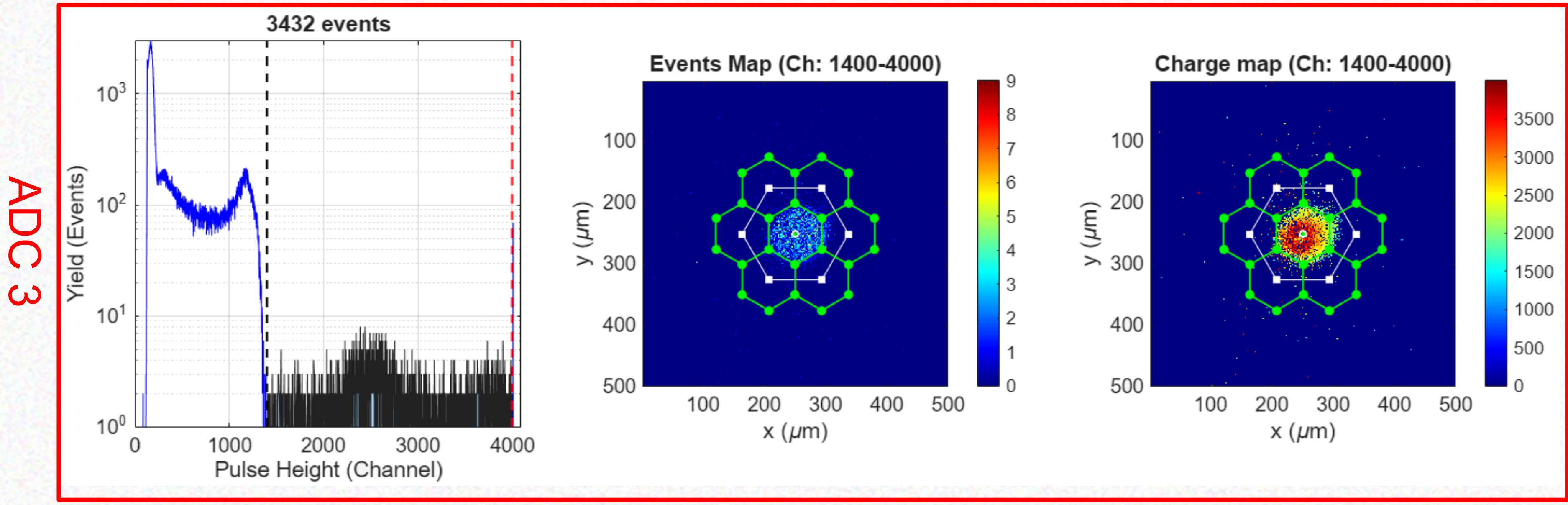

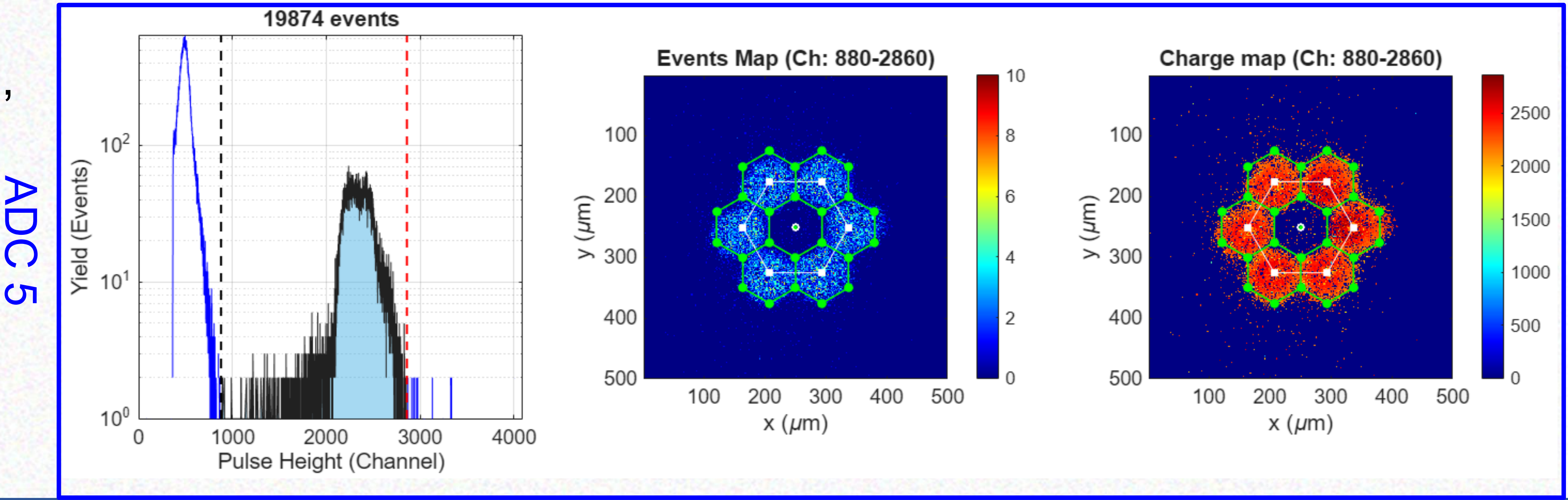

TRIBIC MEASUREMENTS ALONG ONE DEVICE AXIS

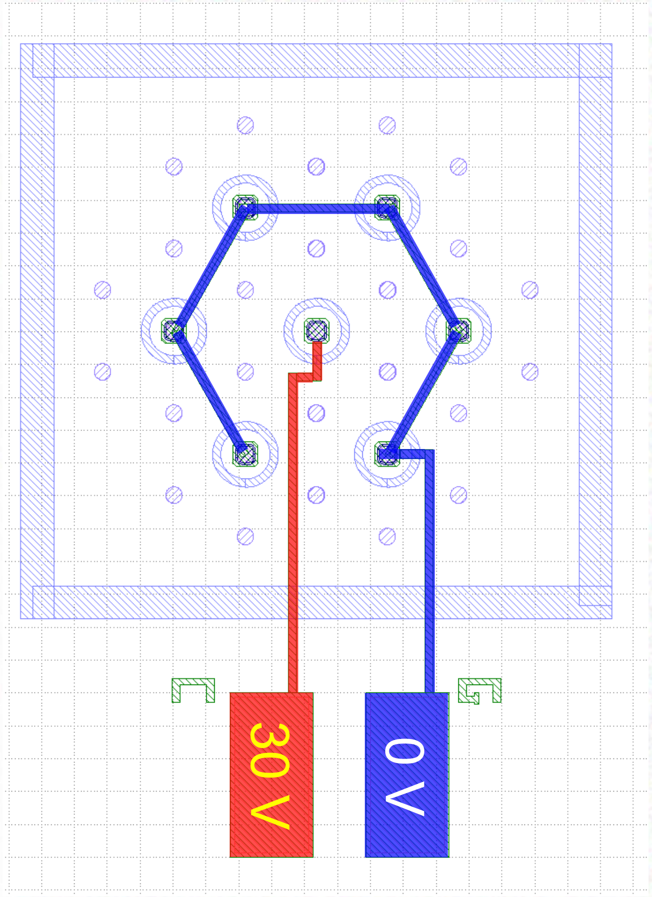

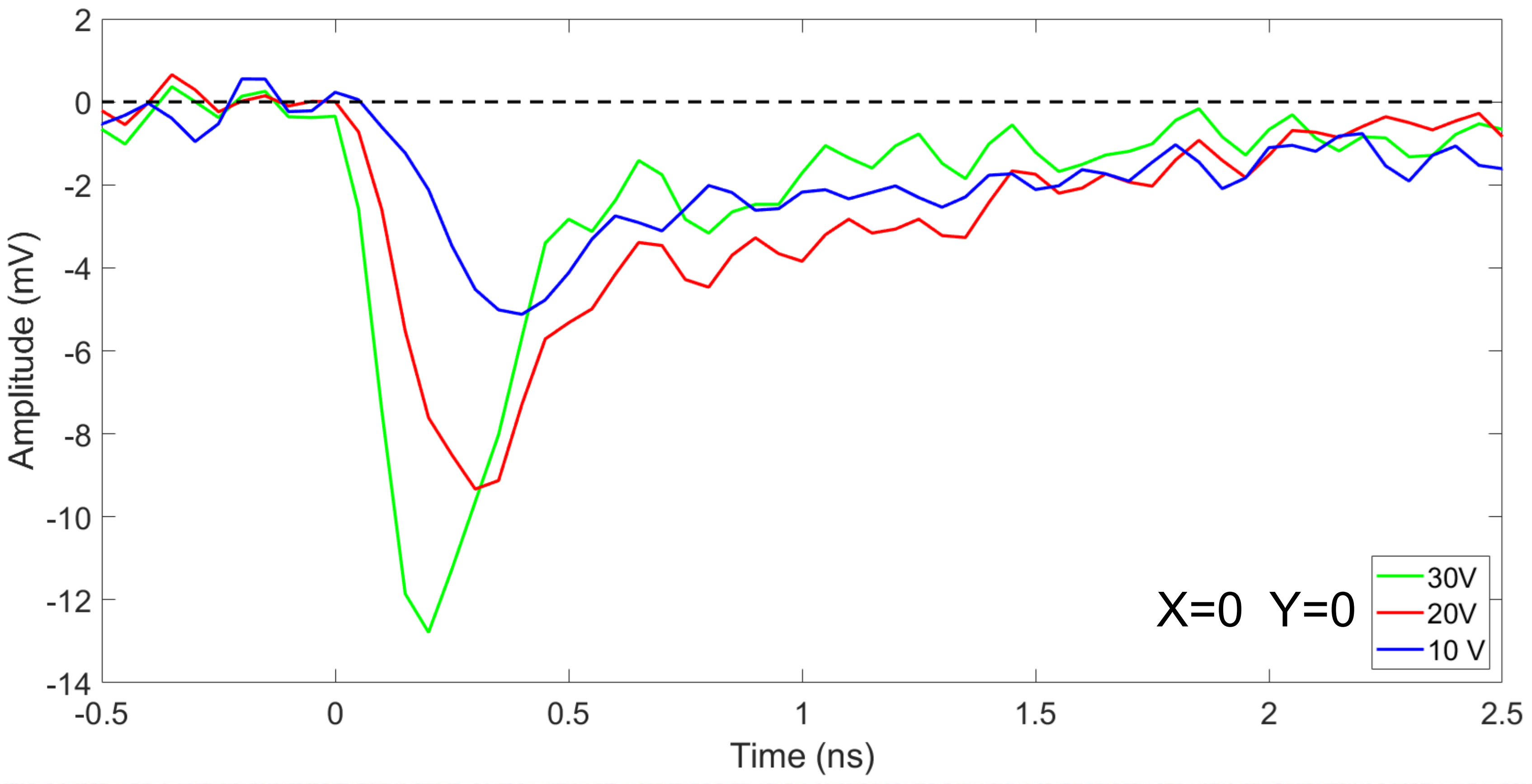

- Puntual shots were carried out along one device axis for TRIBIC measurements, which are currently under analysis.
- Waveform properties like arrival time, rise time, amplitude, and charge are being processed.